DRAFT: Status of ASIAEX Central Simulation

P.J. Haley, P.F.J. Lermusiaux, W.G. Leslie & A.R. Robinson

January 31, 2005 – 4:55 pm

Summary

Many reasonably stable simulations of the 2000 ASIAEX frontal area have been made. In all of them, however, there seems to be an excessive movement of off-shore water onto the shelf (when simulation near-surface salinities are compared to CTD measurements). Current tests are focusing on the initialization procedures.

This document describes the current “best” simulation, run 167, which can be found in `/data2/AOSN2/ASIAEX/PE/2004/Nov22/PJH02`.

Domain

A rotated Cartesian domain is defined in the South China Sea as

$$\begin{aligned} n_x,\ n_y &= 96,\ 120 \\ dx,\ dy &= 1\text{km},\ 1\text{km} \\ lat_c,\ lon_c &= 21.81°\text{N},\ 117.59°\text{E} \\ rotation &= 20.0° \end{aligned}$$

The domain was designed to encompass the shelf/slope SeaSoar survey while keeping the grid boundaries away from potentially troubling topography (figure 1, to right).

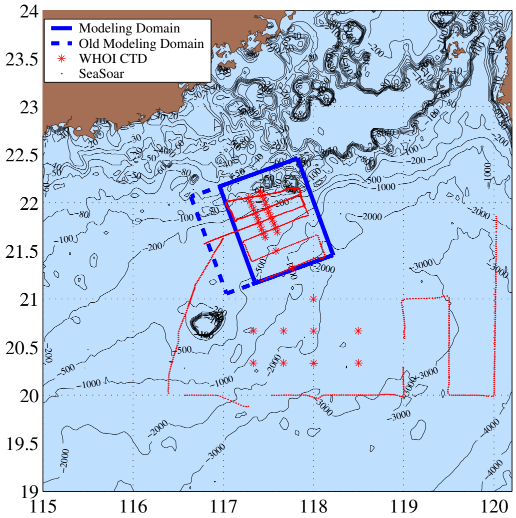

Also shown in figure 1 are the boundaries of the original modeling domain, which extended 35km further to the East. The eastern extent was chosen on the basis of some data that were erroneously identified as coming from the year 2000. This domain is still shown as it is the the basis for cropping the data set to a manageable size.

In the vertical, 39 model levels are spread throughout the water column in a double sigma system (illustrated in figure 2). In addition to overall resolution, special attention was paid to the surface mixed layer (0-26m) and the sub-surface salinity maximum (70-200m).

In Situ Data

The data set was thinned by eliminating any data further than $\frac{1}{60}°$ outside of the original modeling domain. This left 833 SeaSoar pseudo–casts (figures 3-6) spanning the period of 16–18 April 2000 and 24 CTD casts (figures 7-10) on 19 April 2000.

For a further comparison, a search was made for SeaSoar profiles that fell within 3km and 2.5 days of a corresponding CTD profile. An aggregate of 29 SeaSoar profiles were identified as close to one of 6 CTD profiles identified in table 1. Figures 11 and 12 show the comparisons of temperature and salinity between the two instruments. We see both

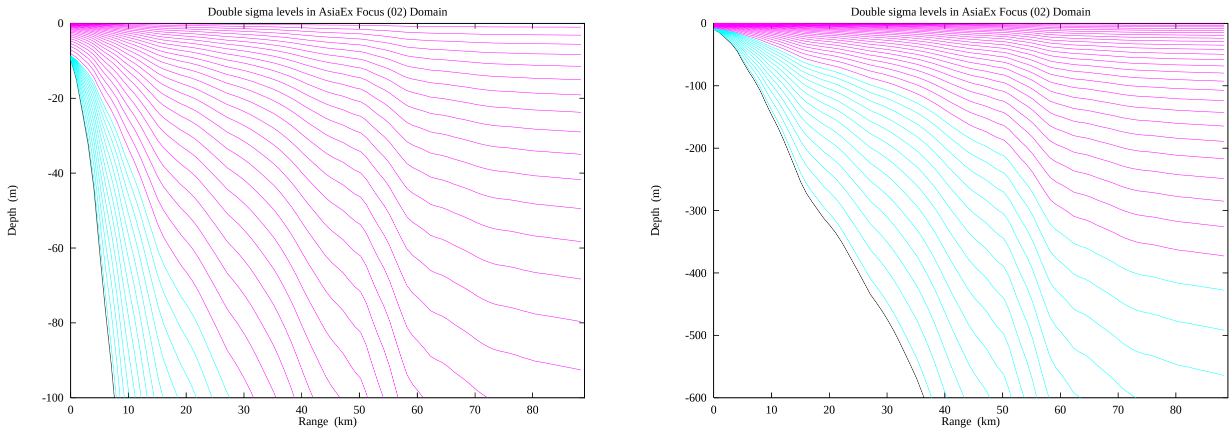

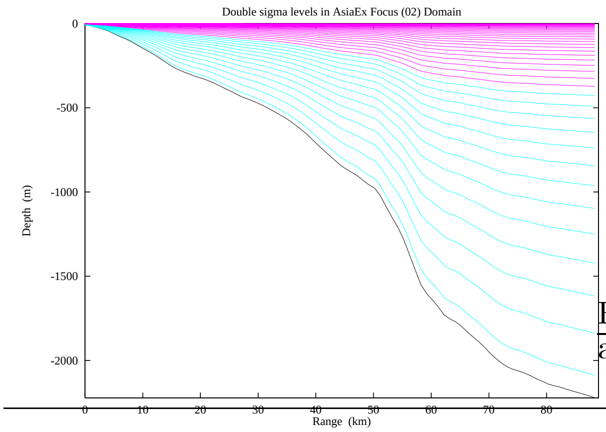

Figure 2 : Double sigma system used in AsiaEx simulations.

Table 1: Nearby CTD/SeaSoar Stations

CTD ID	SeaSoar ID	Separation (km)	Separation (days)		CTD ID	SeaSoar ID	Separation (km)	Separation (days)
10	1210	0.59	1.0000		27	978	0.30	2.3818
10	1209	1.98	0.9941		27	977	0.33	2.3799
10	1211	2.03	0.9893		27	979	0.86	2.3779
11	1154	1.00	1.3994		27	976	0.91	2.3770
11	1155	1.25	1.3945		27	980	1.41	2.3750
11	1153	2.97	1.3887		27	975	1.48	2.3740
13	1112	0.31	1.7168		27	981	1.98	2.3721
13	1111	1.71	1.7129		27	974	2.04	2.3701
13	1113	1.74	1.7080		27	982	2.54	2.3691
18	957	0.26	2.2178		27	973	2.61	2.3672
18	956	0.70	2.2148		32	1104	0.71	2.2002
18	958	1.17	2.2129		32	1103	1.07	2.1963
18	955	1.63	2.2100		32	1105	2.52	2.1914
18	959	2.12	2.2070		32	1102	2.68	2.1875
18	954	2.49	2.2051					

evidence of reasonable inter-calibration between the CTD and SeaSoar, and indications of

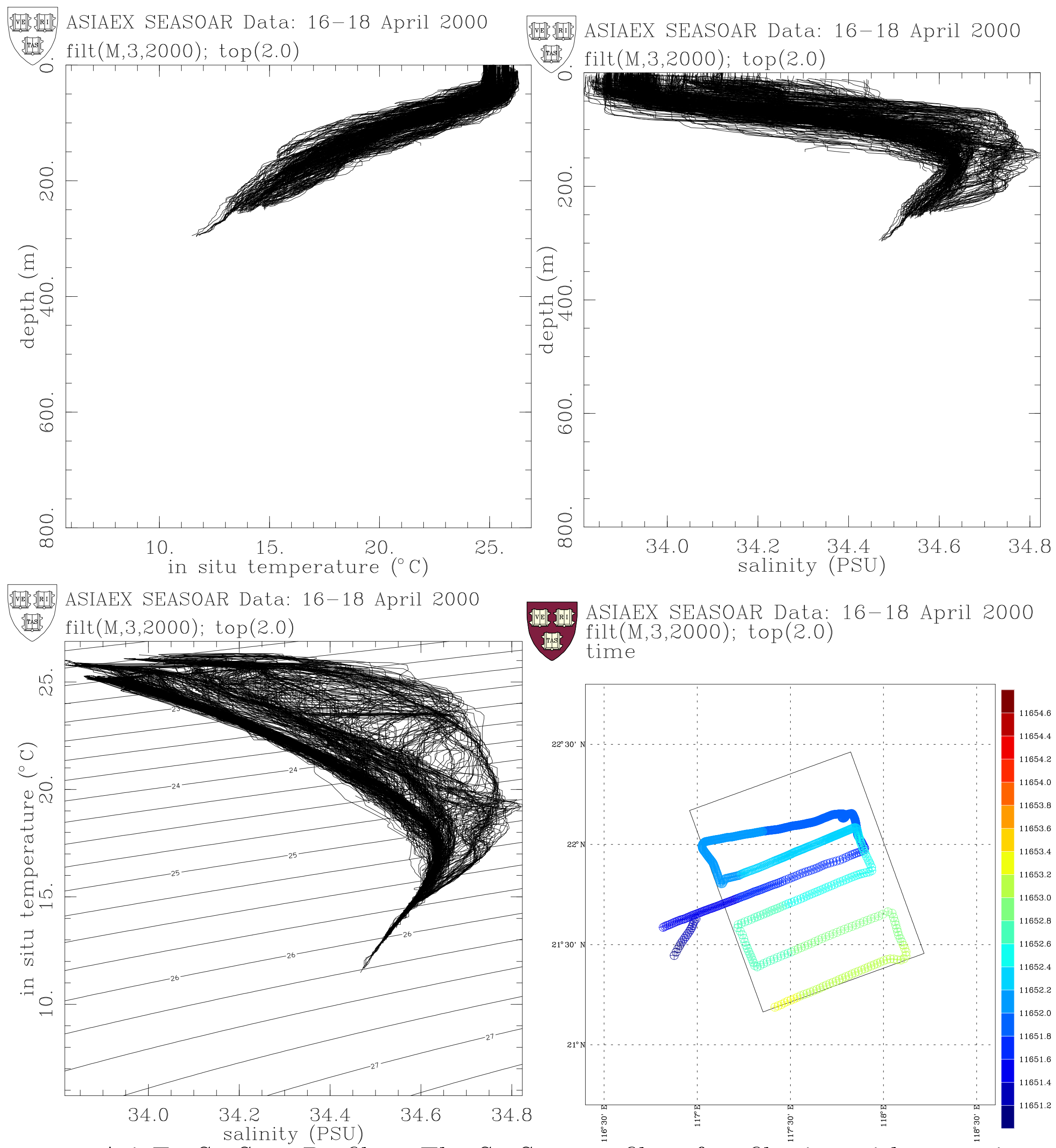

Figure 3 : AsiaEx SeaSoar Profiles. The SeaSoar profiles after filtering with a 3-point median filter and extending any profile within 2m of the surface to the surface.

the speed of evolution of the fields.

Climatology

To fill in around the data, and extend vertically, a 1° annual HydroBase climatology was obtained from the *HydroBase2* Download Database. This was sub-sampled for the

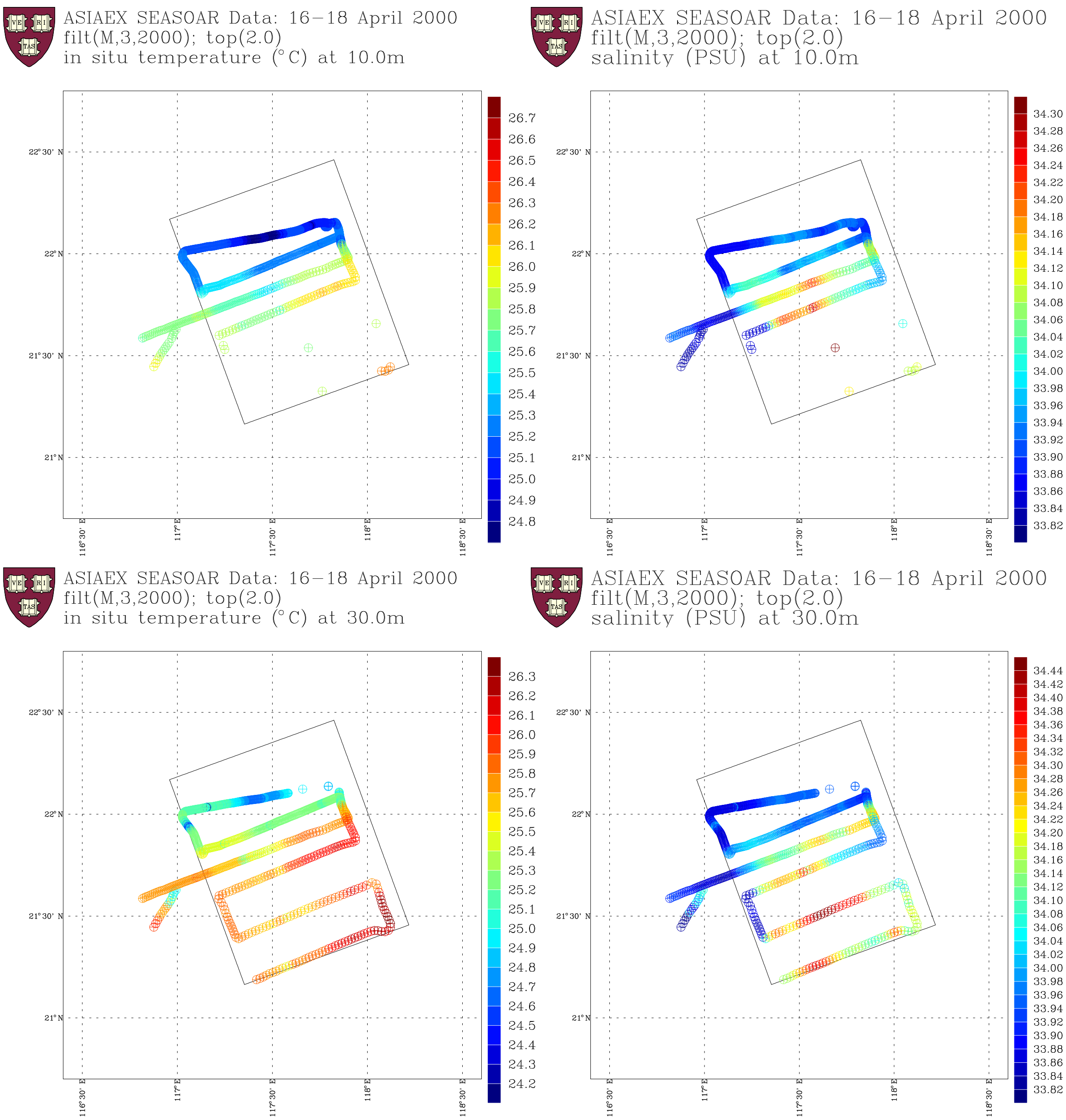

Figure 4 : AsiaEx SeaSoar Points. Top row: in Mixed Layer. Bottom Row: Below mixed layer.

near vicinity of our modeling domain, resulting in 23 profiles. These were further reduced, based on the deep characteristics (see Initialization section), to 16 profiles (figures 13-16).

Atmospheric Forcing

From the Master Environmental Library, we obtained the atmospheric forcing fields for the period April 12–21, 2000 indicated in table 2.

From the full set of atmospheric fields, a "best" subset of 6 hourly fields spanning

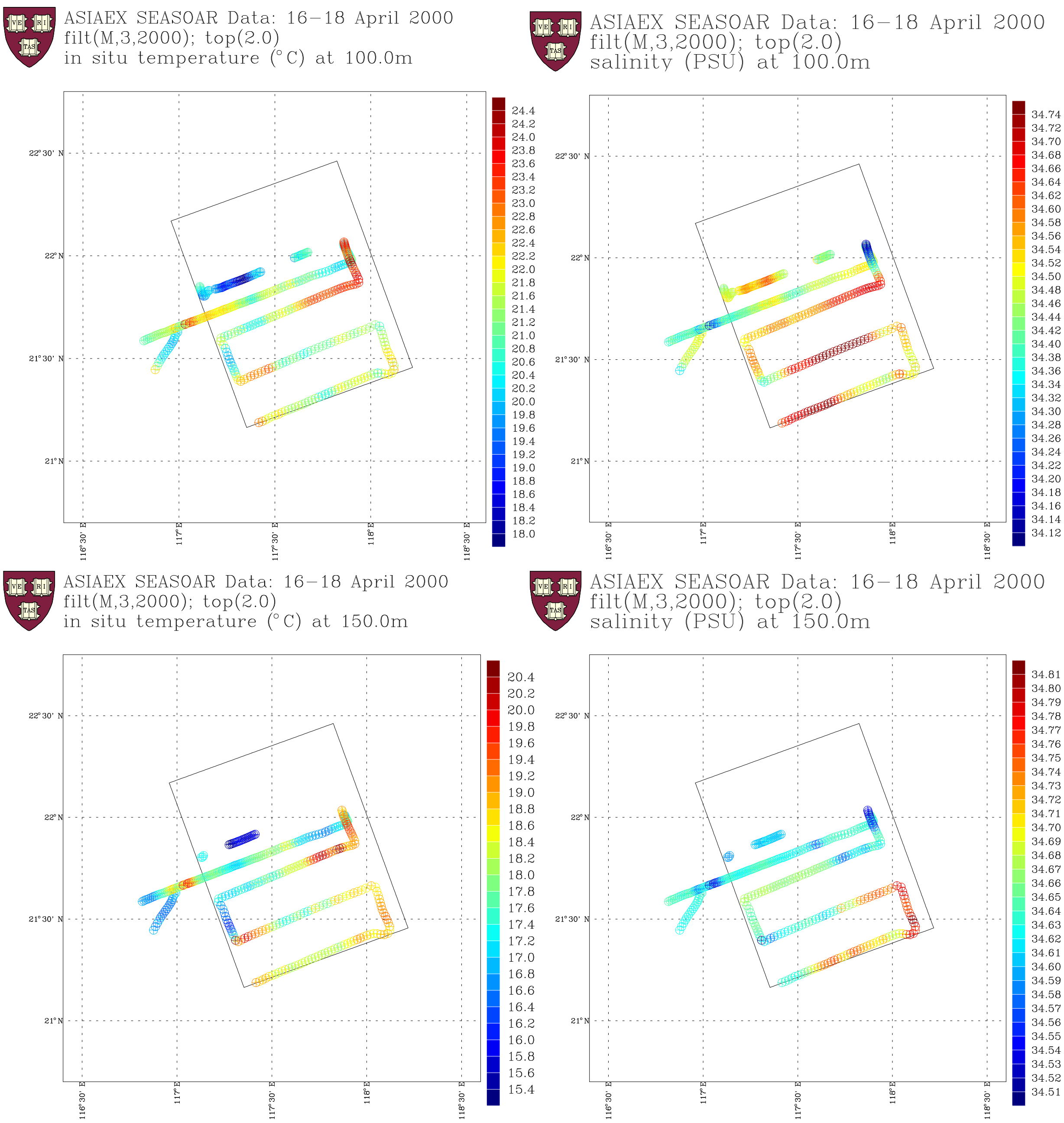

Figure 5 : AsiaEx SeaSoar Points. Top row: Main thermocline. Bottom Row: Salinity maximum.

the period 14 April 0000Z – 21 April 0000Z are chosen. Since this is a two step process with a full set of data required at every time, the various discrepancies in issuance and forecast frequency can results in some mismatches, as shown in figure 17. These fields are combined with an analytic expression for incident solar radiation and bulk formulae to produce pseudo-hourly net heat flux, evaporation minus precipitation, wind stress and solar radiation at the ocean surface. Finally these fields are interpolated onto the model horizontal grid. The resulting wind stress are shown in figure 18 at the original forecast

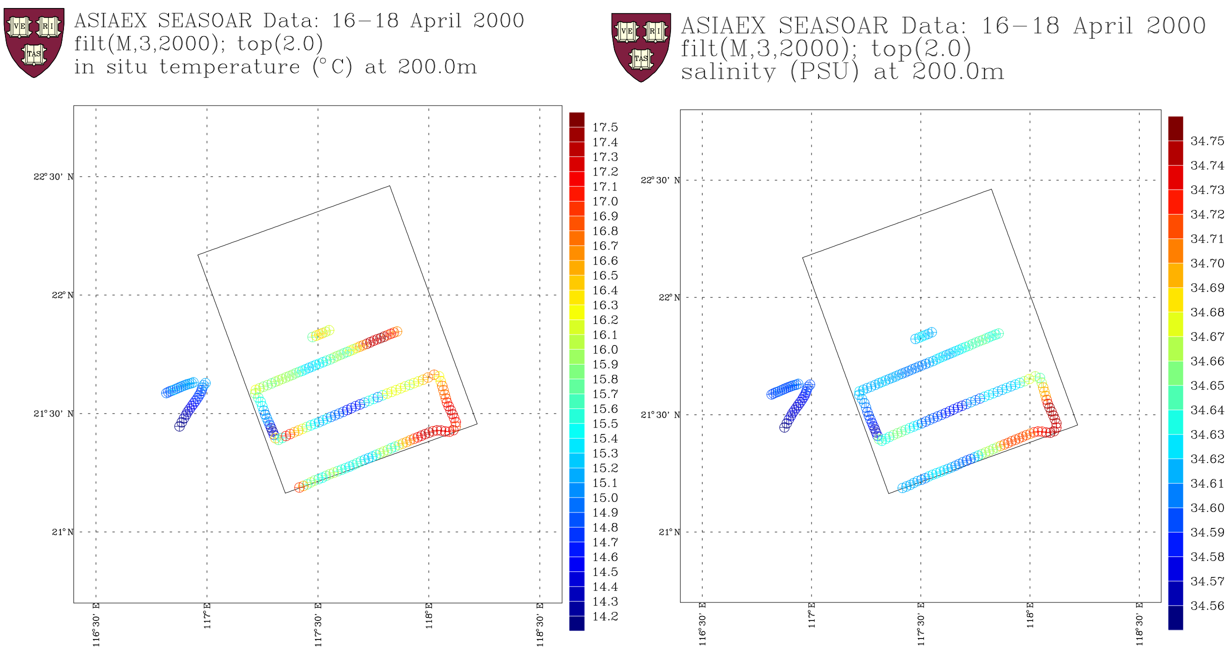

Figure 6 : AsiaEx SeaSoar Points. “Deep” data.

Table 2: atmospheric forcing fields

	Wind Speed	**Cloud Cover**	**Air Temp–erature**	**Relative Humidity**	**SST**	**Pressure**	**Precip–itation**
Source	COAMPS	NOGAPS	COAMPS	COAMPS	TOPS	COAMPS	COAMPS
Spatial Resolution	0.2°	1° (1)	0.2°	0.2°	1° (1)	0.2°	0.2°
Temporal Resolution	6 hr	12 hr	6 hr	6 hr	6 hr	6 hr (2)	6 hr
Forecast Duration	3 days	5 days	3 days	1 day	3 days	3 days	3 days
Issued	0600 1800	0000 1200	0600 1800	0600 1800	0000 1200 (3)	0600 1800	0600 1800
Last Analysis	4/18 1800	4/19 0000	4/18 1800	4/18 0600	4/19 0000	4/18 1800	4/18 1800 (4)

(1) Original resolution. These fields were bi–cubically interpolated to a 0.2° grid.
(2) No pressure forecasts for 24-42hr
(3) No SST forecasts issued on 1200Z, just analyses
(4) There is never a precipitation analysis, just a 6hr forecast.

temporal resolution.

Initialization

The SeaSoar data were objective analyzed at a central time of Julian day 11650.674 (15 Apr 2000 - 16:10:33) (local midnight) with the OA scales shown in table 3. (Note that

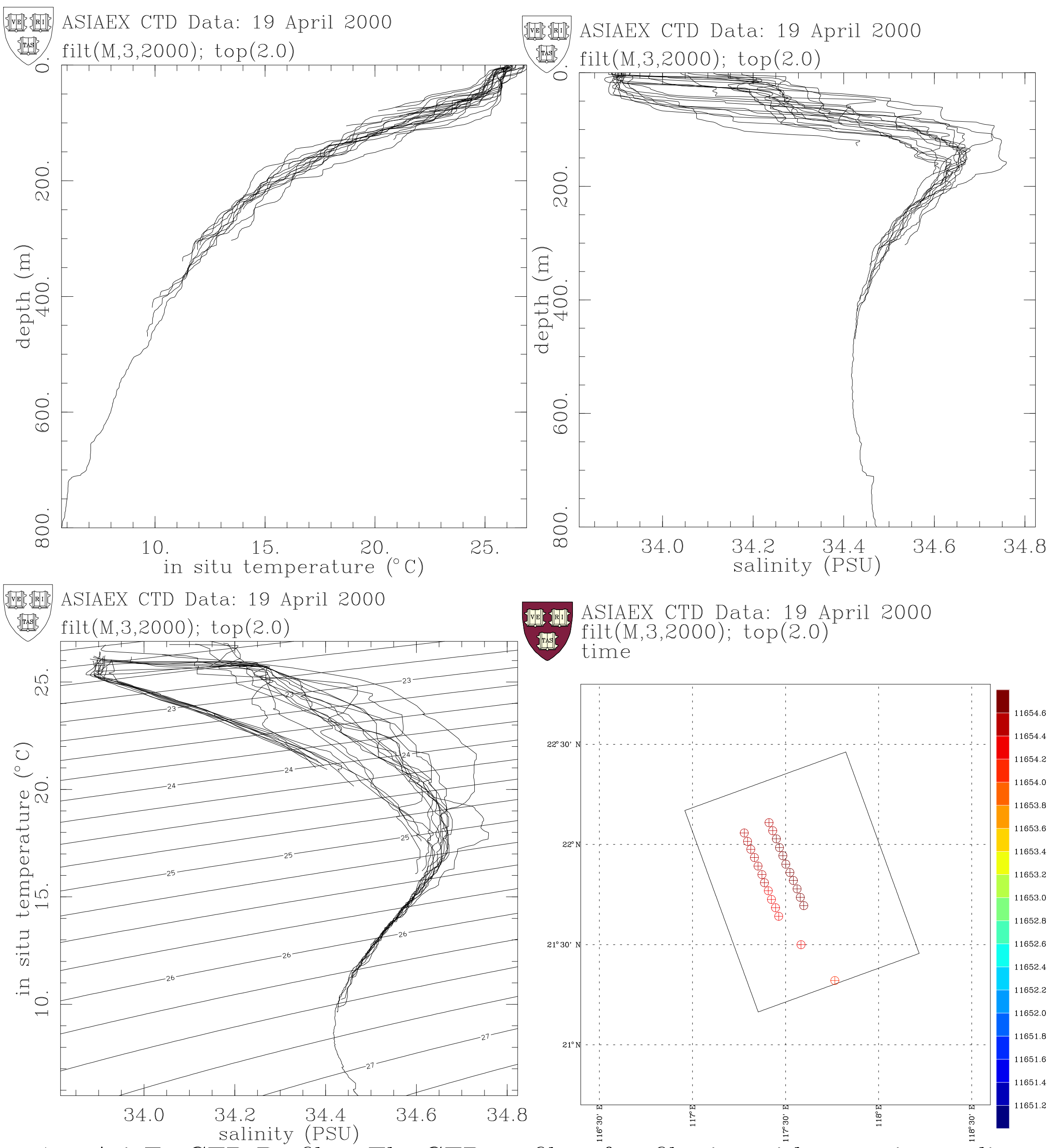

Figure 7 : AsiaEx CTD Profiles. The CTD profiles after filtering with a 3-point median filter and extending any profile within 2m of the surface to the surface.

the OA was made before the domain was restricted and before the HydroBase climatology was found.) The surface salinity from that analysis is shown in figure 19. In the eastern portion of the domain a surface salinity front is evident which extruded off-shore in the western third of the domain. This extrusion may be valid for the initial field or may be the result of extending a line of data ∼3 days after the central date (figures 3 & 4). To

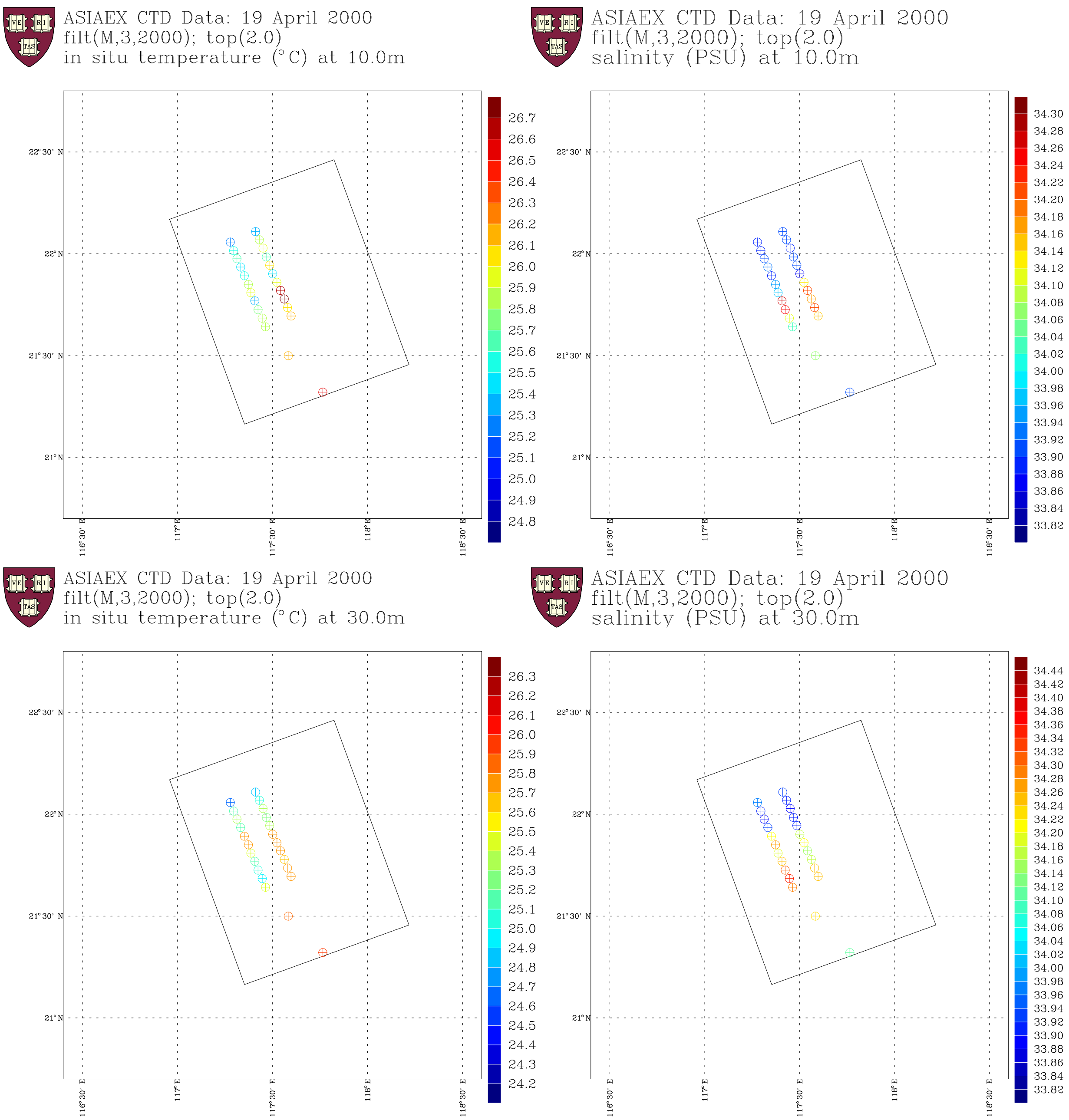

Figure 8 : AsiaEx CTD Points. Top row: in Mixed Layer. Bottom Row: Below mixed layer.

test this, a temperature/salinity based feature model of a shelf/slope system (originally developed for the middle Atlantic Bight) was used.

Table 3: OA Scales

	Synoptic	Mean
Decay (km)	25	250
Zero-Cross (km)	50	500
Time-Decay (day)	4	1000

The first step was to segregate the data profiles into shelf/off-shelf groupings. A profile was identified as being a "shelf" profile if either of the following conditions was true:

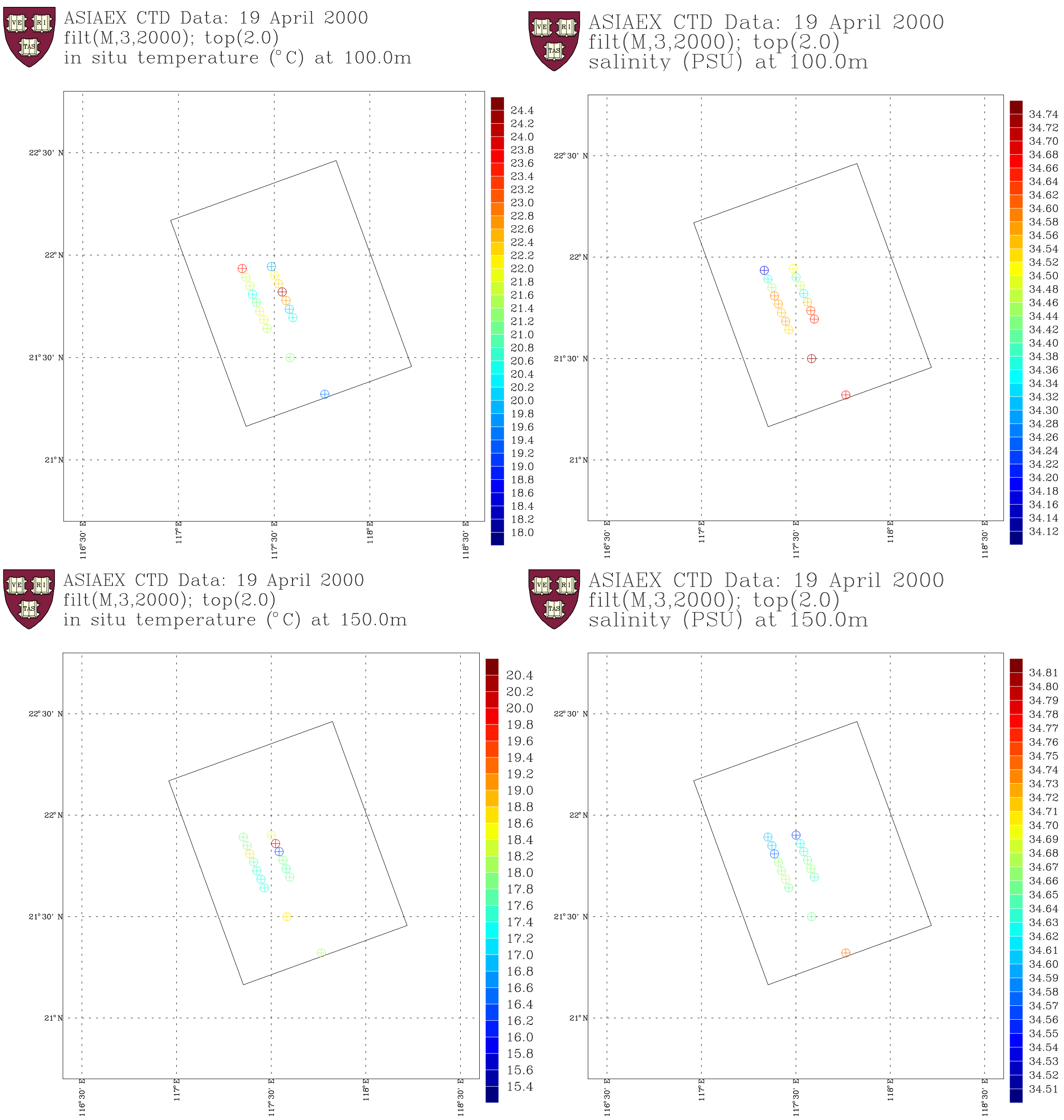

Figure 9 : AsiaEx CTD Points. Top row: Main thermocline. Bottom Row: Salinity maximum.

(i) the salinity at 30m was less than or equal to 34.05 PSU

(ii) the salinity at 100m was less than or equal to 34.26 PSU.

The set of "off-shelf" profiles was made from the union of:

(a) profiles not included in the "shelf" set

(b) portions of the "shelf" profiles at or below 150m.

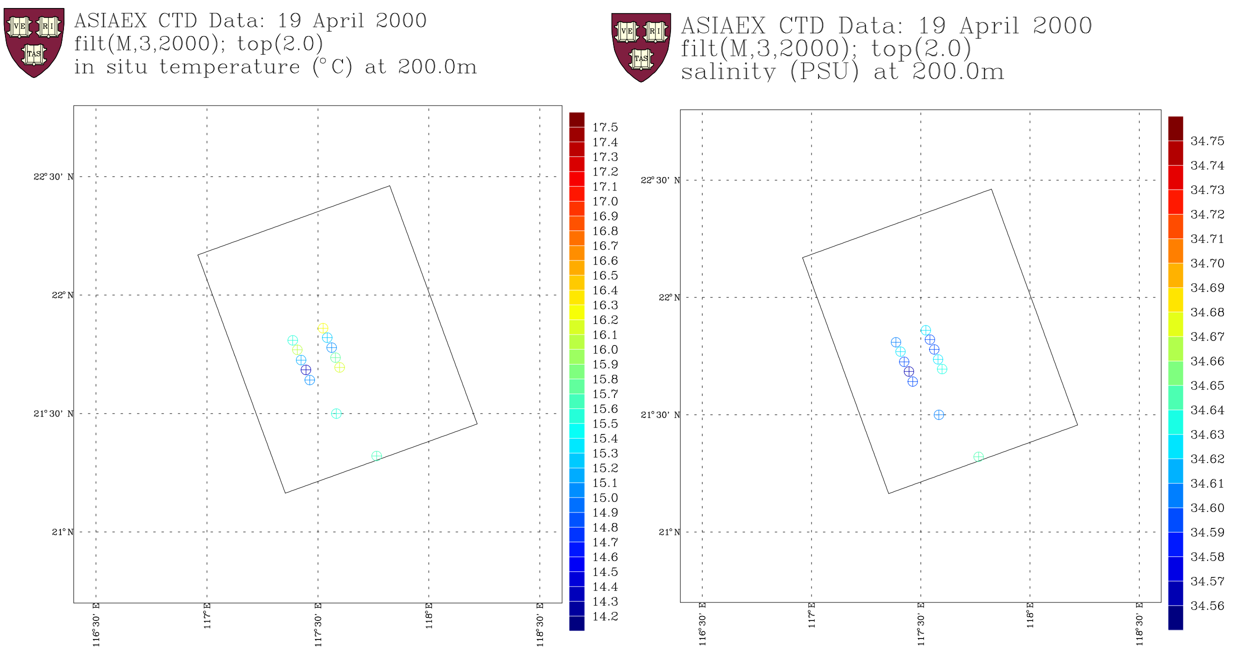

Figure 10 : AsiaEx CTD Points. "Deep" data.

Table 4: OA Scales

	Synoptic	Mean
Decay (km)	12.5	125
Zero-Cross (km)	25	250
Time-Decay (day)	4	1000

The initial fields were created by melding 2 objective analyses at a central time of Julian day 11650.674 (15 Apr 2000 - 16:10:33) (local midnight) with the OA scales shown at right. The first analysis was of the SeaSoar "shelf" profiles alone. The second analysis combined the SeaSoar "off-shelf" data with a selected portion of the HydroBase climatology and CTD profiles to fill-in at depth. The HydroBase profiles were limited by the following criteria:

(1) Profiles with a salinity greater that 34.438 PSU at 500m were discarded to provided better agreement with the limited deep CTD data.

(2) All HydroBase data shallower than 120m were discarded to avoid coarse vertical resolution in the surface layers.

The CTDs were limited by discarding all data shallower than 150m.

The OAs were melded across a front which needed to be defined. From a data analysis by Wayne Leslie, the foot of the front is assumed to lie along the 110m isobath. This curve was compared to the 34.05 surface salinity contour from the exploratory OA (figure 19). Only the portion east of 117.4E was retained. The mean distance between this surface curve and the frontal foot was determined (4.798km). A contour 4.798km off-shore of the 110m isobath was generated and used as the surface expression of the front[1]. This gives a mean slope of 0.023. For the melding procedure, the slope of the front is allowed to vary in the range [0.01 0.08]. The e-folding half width of the front is 6.25km. The results of this melding can be seen in `/data/projects/ASIAEX/FM/2004/Sep01/PJH01`.

[1] Also considered, and plotted, was the surface temperature contour made from the median temperature (25.3574 °C) along the chosen surface expression.

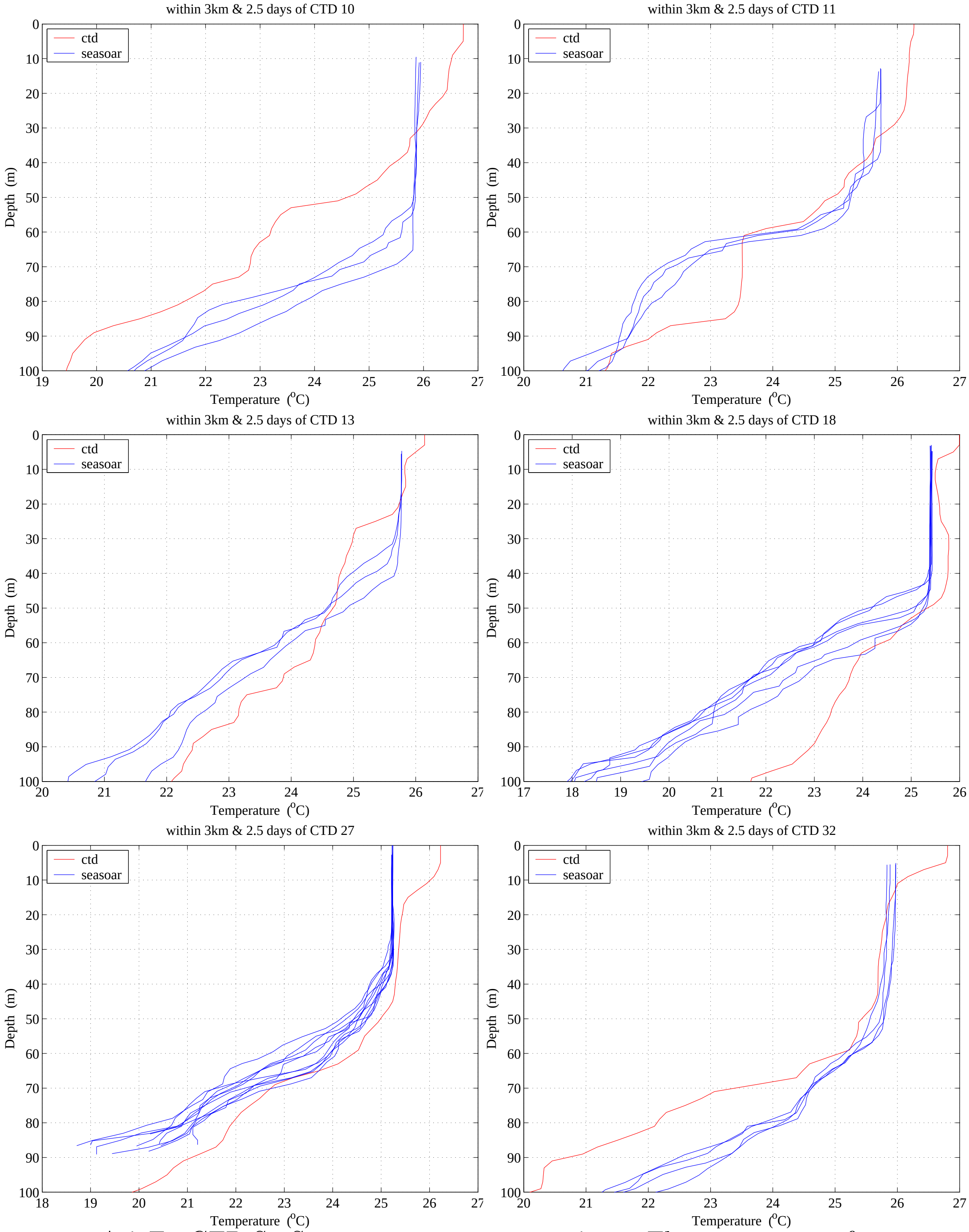

Figure 11 : AsiaEx CTD-SeaSoar temperature comparison. The temperature from any CTD which has SeaSoar profiles within 3km and 2.5 days is plotted along with the nearby SeaSoar temperatures.

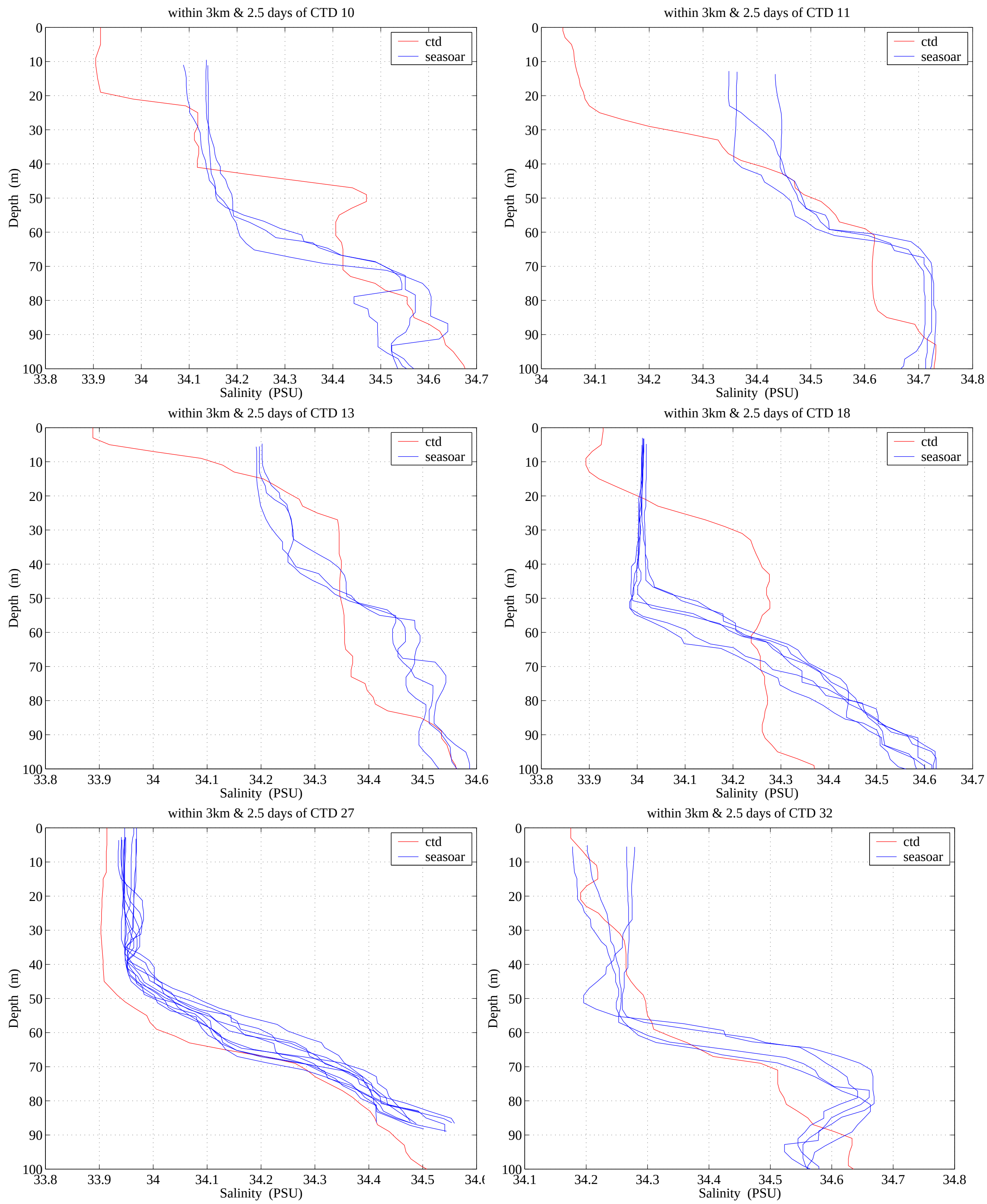

Figure 12 : AsiaEx CTD-SeaSoar salinity comparison. The salinity from any CTD which has SeaSoar profiles within 3km and 2.5 days is plotted along with the nearby SeaSoar salinities.

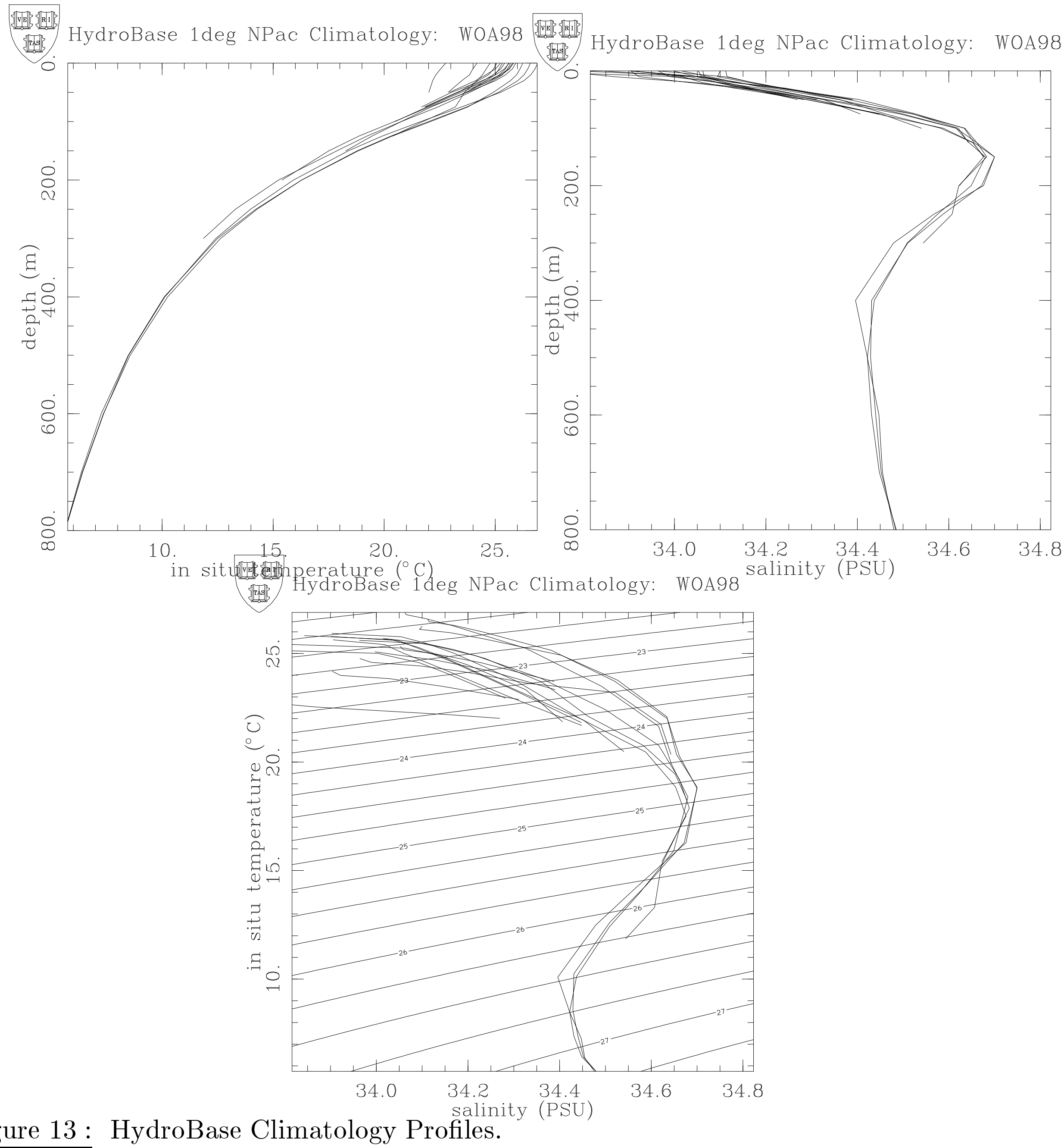

Figure 13 : HydroBase Climatology Profiles.

"Terminal" conditions were generated using the same procedure on the CTD data at the central Julian date of 11654.674 (19 Apr 2000 - 16:10:33) (local midnight).

These initial and terminal fields were processed through PE_initial to produce initialization and time varying boundary data. Initial & boundary velocities were generated from geostrophy. A series of reference surfaces (50m, 100m, 150m, 300m, 500m, 1000m, 2000m, the estimated depth of the salinity maximum and the bottom terrain-following level) were tested. The resulting transport streamfunctions and 30m velocity fields are displayed in

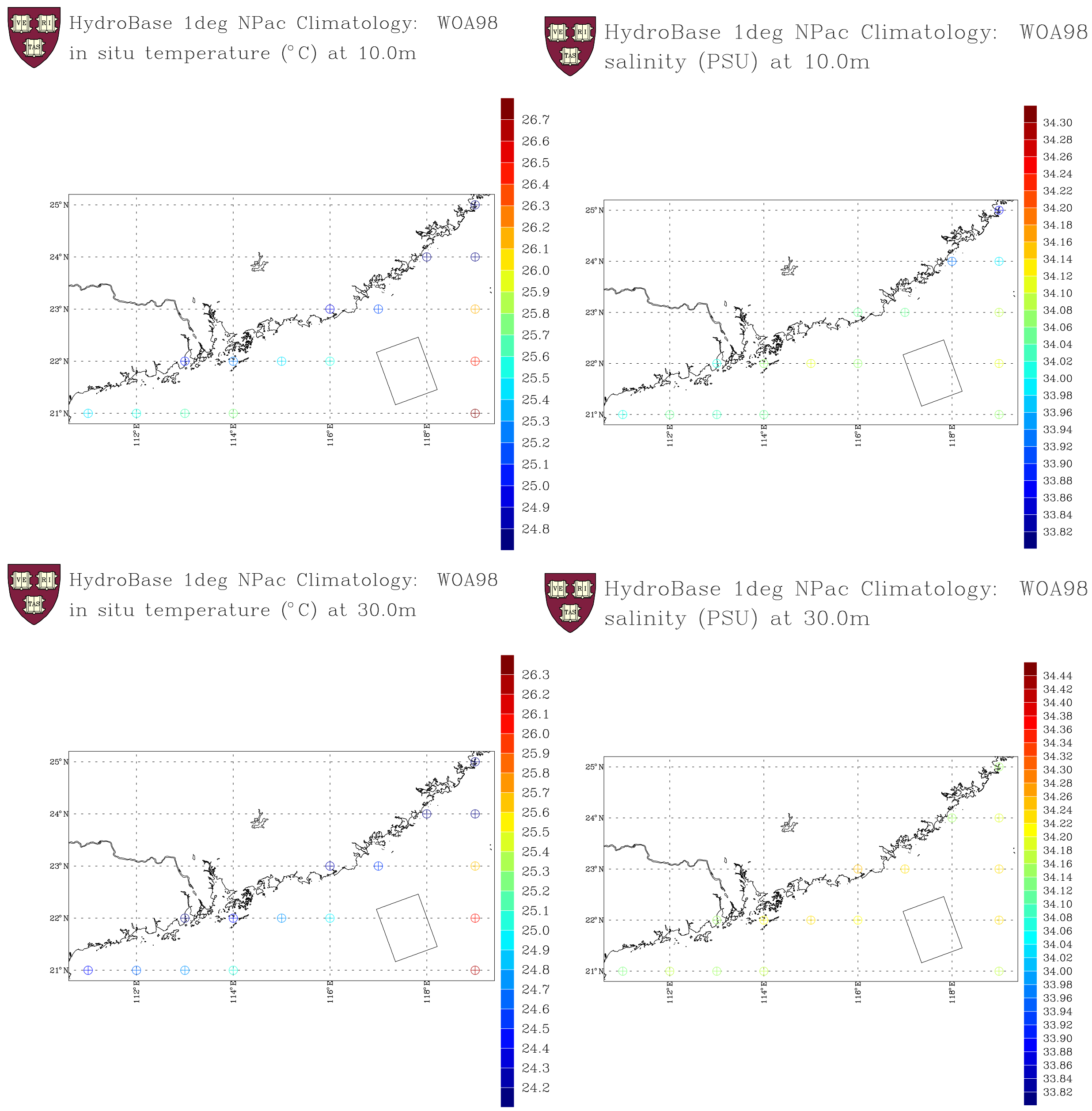

Figure 14 : HydroBase Climatology Points. Top row: in Mixed Layer. Bottom Row: Below mixed layer.

figures 20 and 21 respectively. Deepening the reference surface reduces the initial transport at the expense of increasing the near surface velocity. The best compromise was found to be a reference surface based on the depth of the salinity maximum (figure 22).

Assimilation

The assimilation fields were more straight-forward. Since the assimilation only uses

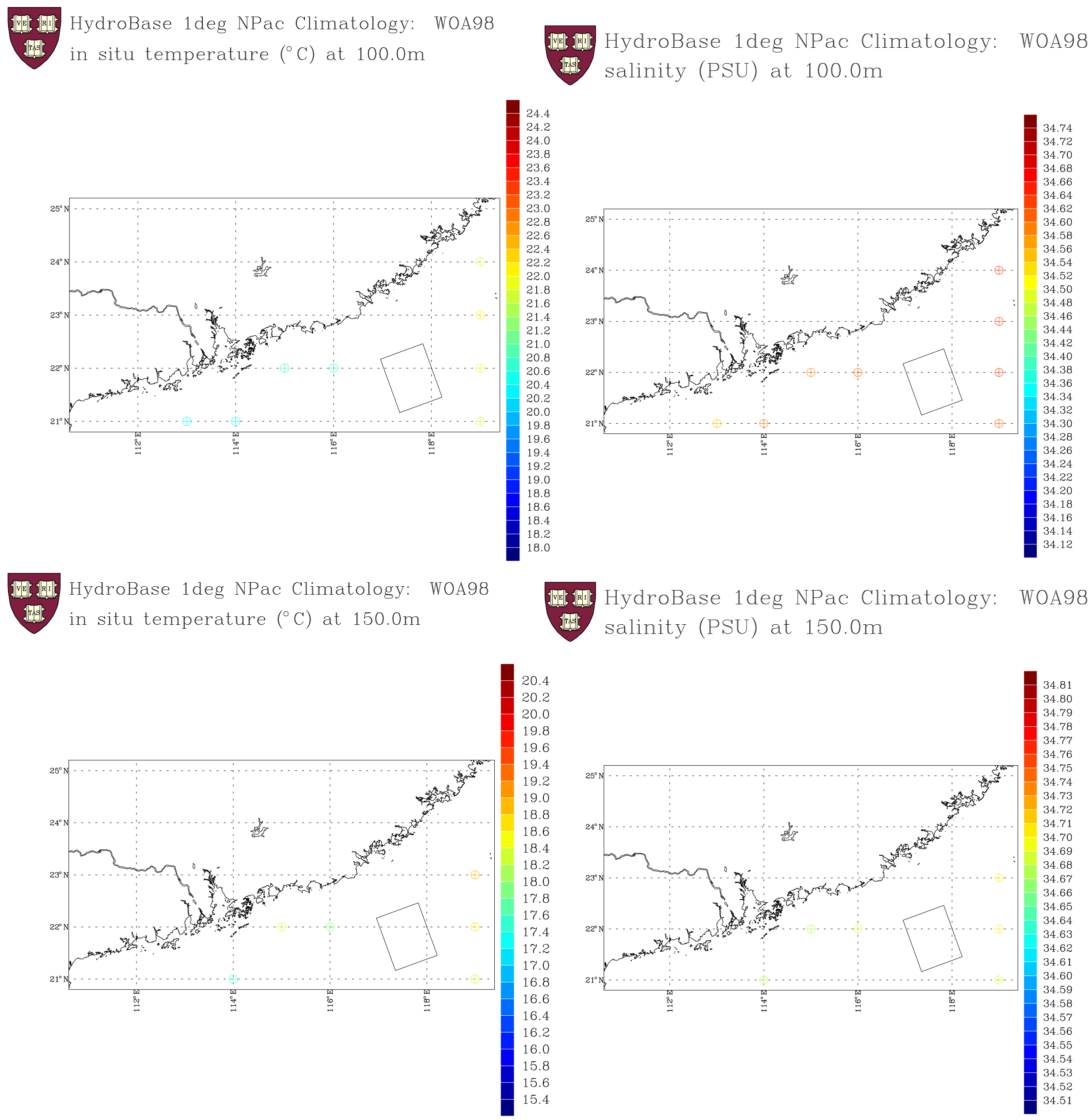

Figure 15 : HydroBase Climatology Points. Top row: Main thermocline. Bottom Row: Salinity maximum.

Table 5: OA Scales

	Synoptic	Mean
Decay (km)	6.25	62.5
Zero-Cross (km)	12.5	125
Time-Decay (day)	0.5	1000

the low error portion of the fields, the feature model formalism was not used. Regular OAs of the SeaSoar and the CTD data were made at half day intervals with the parameters at right. For the SeaSoar, assimilation OAs were made twice daily between Julian dates 11651.174 – 11653.174. For CTDs, the assimilation OAs were made on Julian dates 11654.174 & 11654.674. The concatenated

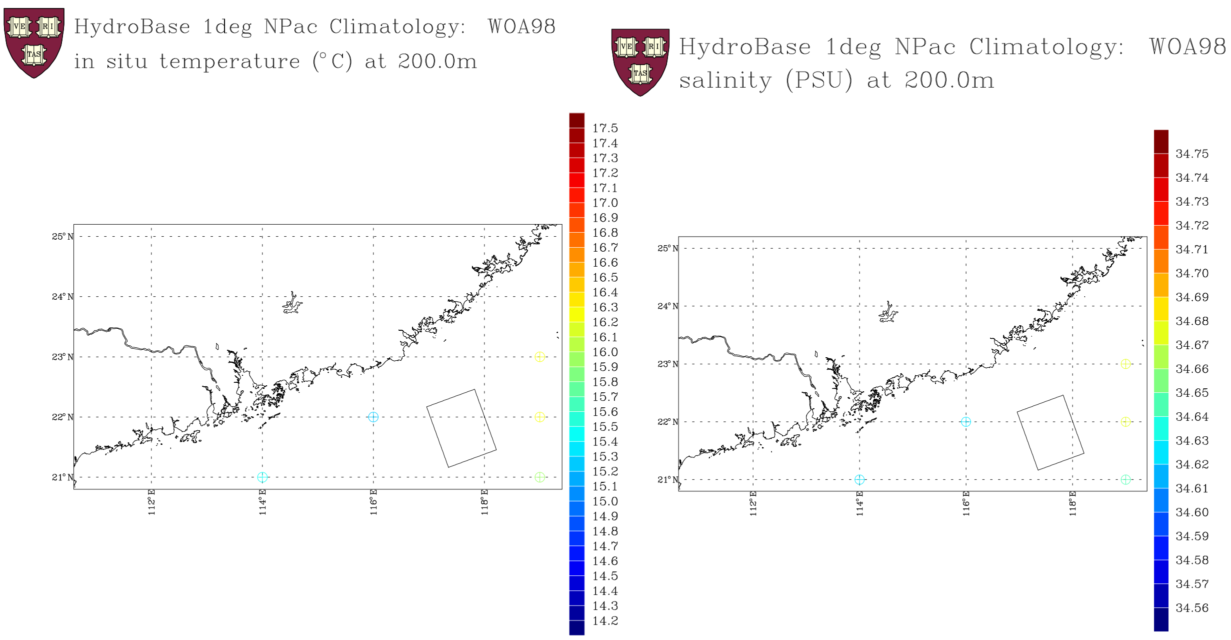

Figure 16 : HydroBase Climatology Points. "Deep" data.

results can be viewed in `/data/projects/ASIAEX/PE_initial/2004/Sep01/PJH02`.

The fields that were actually assimilated were internal mode velocity, temperature and salinity. They were assimilated with the ramping weights at right.

Table 6: OI Ramping

Time (day)	T/S	u',v'
τ-0.125	0.3	0.15
τ-0.0625	0.6	0.3
τ	0.9	0.45

Mixed Layer Model

To choose the mixed layer model & parameters, we begin by examining the *in situ* data and the atmospheric forcing. Mixed layer depth data are obtained by computing the potential density anomalies, σ_θ, for the SeaSoar and CTD profiles. The mixed layer depth, z_{mld}, for a each profile is then defined as the shallowest depth where $|\sigma_\theta(z_{mld}) - \sigma_\theta(0)| > 0.01\ \left(\mathrm{kg/m^3}\right)$ (figure 23).

Table 7: MLD Fitting

	Bias (m)	RMS (m)
Ekman	-0.19771	12.2102
Niiler-Kraus	1.4827	15.5727

In the PE model, a mixed layer depth prediction is made based on the atmospheric forcing. The two model choices are

(1) an "Ekman" model

$$Z^E_{mld} = \kappa_E \frac{||\tau||}{\rho f}$$

where κ_E is an adjustable constant, $||\tau||$ is the magnitude of the wind stress, ρ is the density of sea water at the surface, and f is the coriolis.

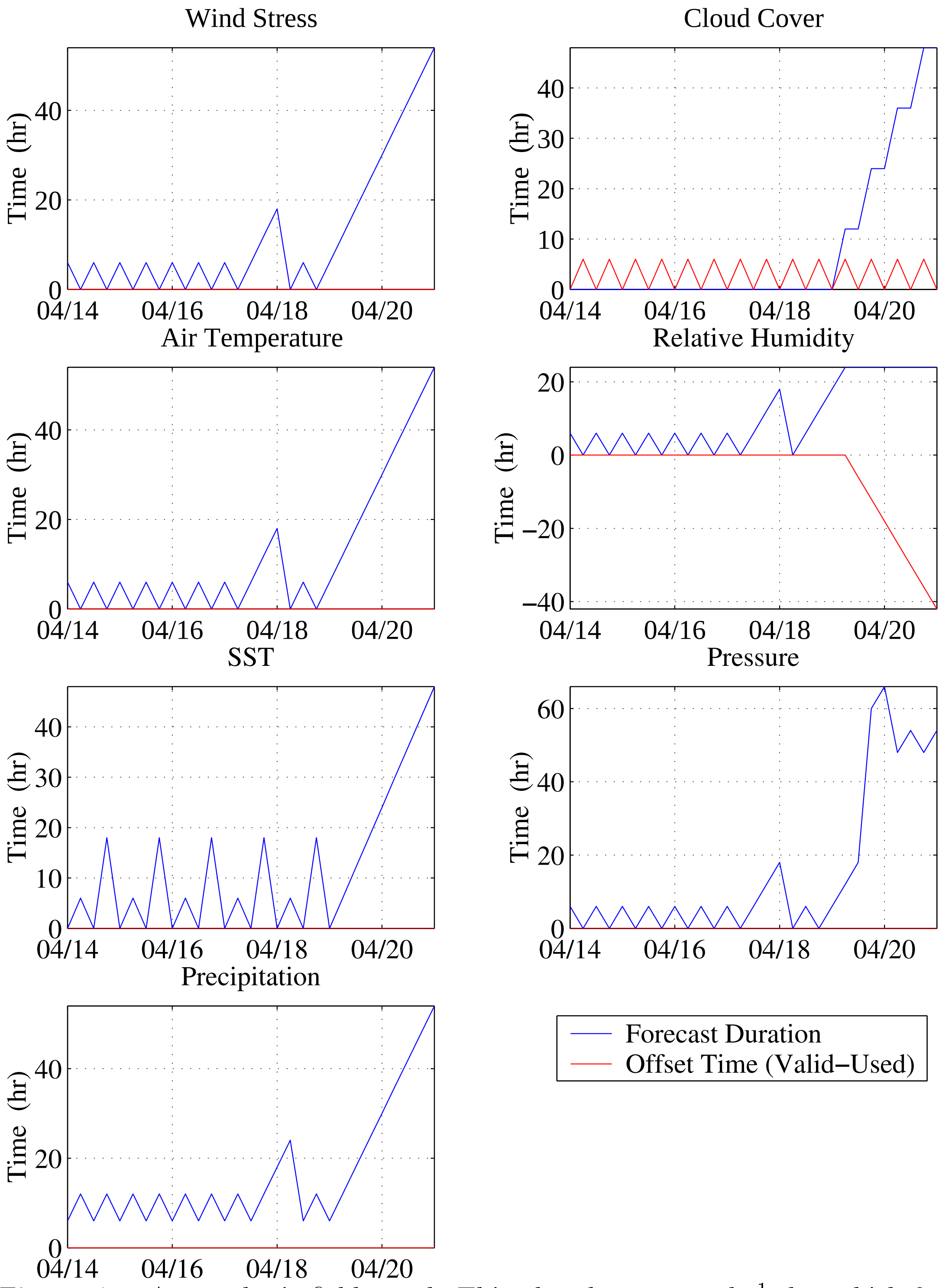

Figure 17 : Atmospheric fields used. This plot shows at each $\frac{1}{4}$ day which forecasts were used (zero duration implied analysis used) and any disparity between the times at which the analyses/forecasts are valid and the times at which they are used.

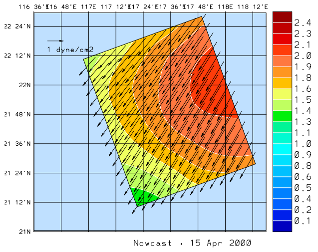

15 Apr 1200

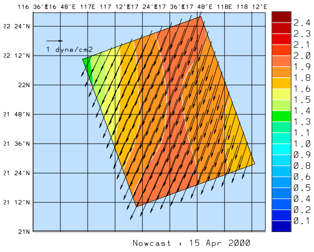

15 Apr 1800

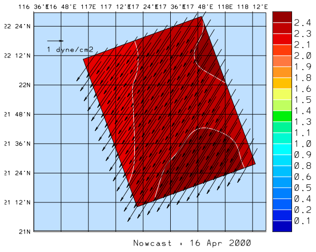

16 Apr 0000

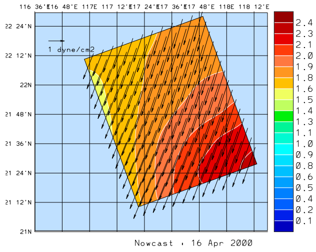

16 Apr 0600

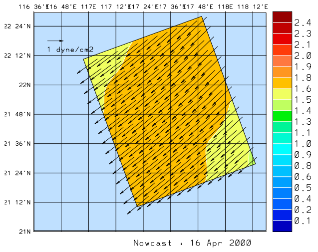

16 Apr 1200

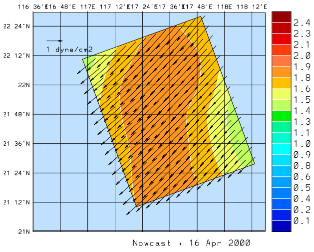

16 Apr 1800

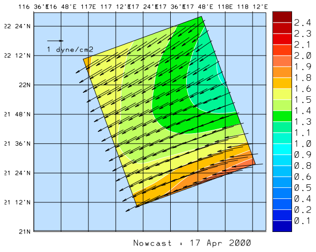

17 Apr 0000

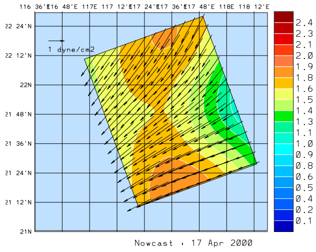

17 Apr 0600

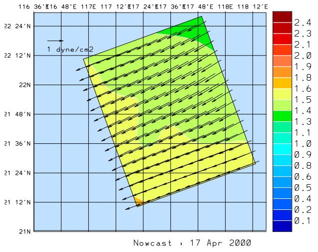

17 Apr 1200

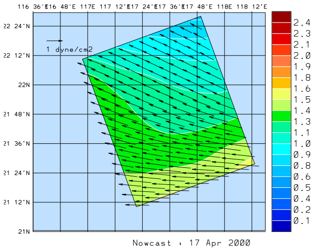

17 Apr 1800

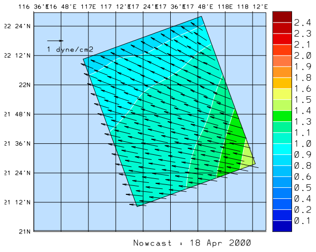

18 Apr 0000

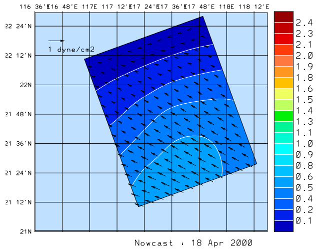

18 Apr 0600

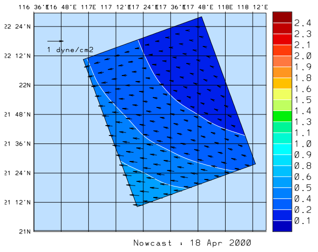

18 Apr 1200

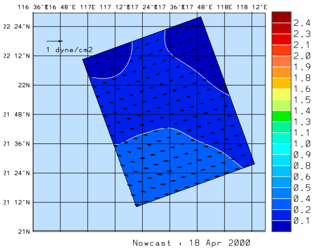

18 Apr 1800

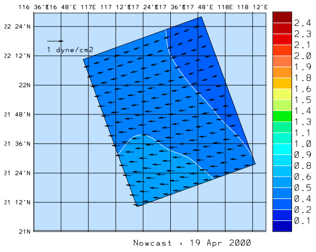

19 Apr 0000

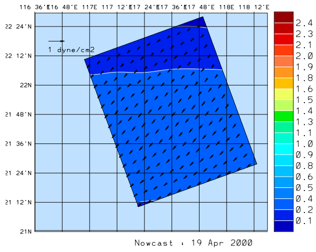

19 Apr 0600

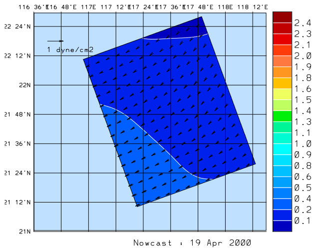

19 Apr 1200

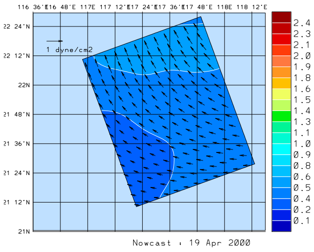

19 Apr 1800

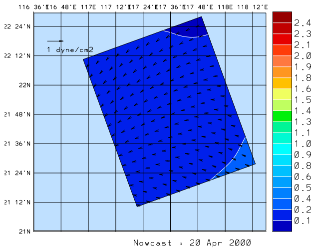

20 Apr 0000

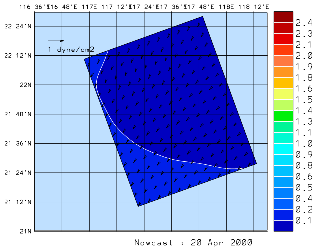

20 Apr 0600

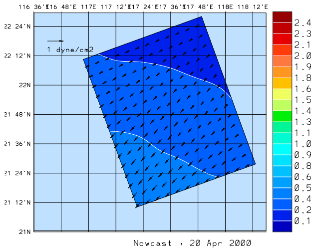

20 Apr 1200

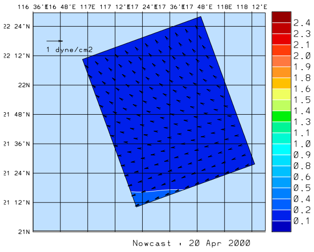

20 Apr 1800

Figure 18 : Wind Stress fields directly affecting AsiaEx simulation. Below: speeds in knots, stresses in dynes/cm^2.

Speed		1.0		3.5		6.5		10.5		16.5		21.5		27.5
Stress		0.0048		0.059		0.20		0.53		1.31		2.2		3.6
Beaufort	0		1		2		3		4		5		6	

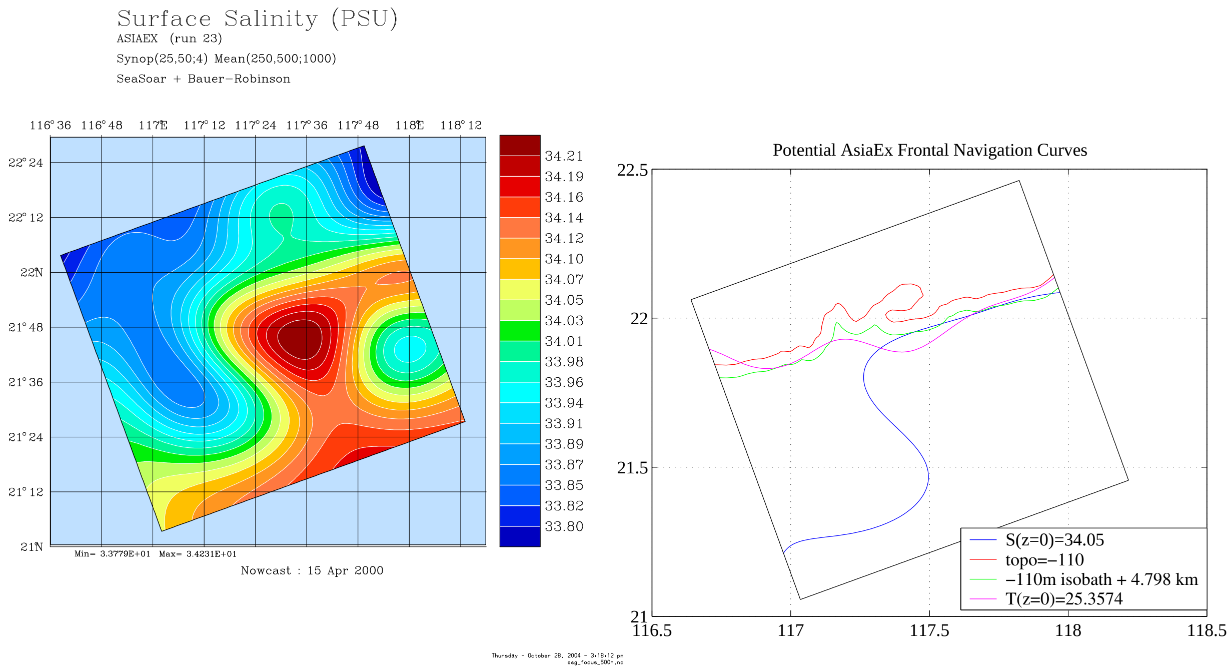

Figure 19 : Constructing shelf/slope front. Left: Surface salinity from an objective analysis of all SeaSoar data. Right: Various curves used to define the shelf/slope front.

(2) a model based on Niiler & Kraus (1977)

$$Z_{mld}^{NK} = 2\frac{M||\tau||^3 - \frac{g\alpha}{\gamma_{H_2O}}Q_I}{-g\alpha Q_I - [(1+N)B - (1-N)|B|]}$$

where M & N are adjustable constants, g is the acceleration due to gravity, α is the thermal expansion coefficient, γ_{H_2O} is the attenuation of light in sea water (taken to be $4\left(10^{-4}\right)\,\mathrm{cm}^{-1}$), Q_I is the incident solar radiation (with the convention here that fluxes out of the water are positive), and B is the net buoyancy flux given by

$$B = -g\alpha Q_{net} - g\alpha Q_I + g\beta E$$

where Q_{net} is the net heat flux, β is the saline contraction coefficient, and E is the evaporation minus precipitation.

From the *in situ* data, we can evaluate ρ, α and β based on surface values; evaluate f and g based on the latitude. From the atmospheric forcing, we can interpolate $||\tau||$, Q_I, Q_{net} and E to the profile positions. Instead of interpolating the fluxes to the profile times, T, we average them as

$$\langle Q\rangle = \frac{\int_{T-T^*}^{T} e^{(t-T)/\tau} Q\,dt}{\int_{T-T^*}^{T} e^{(t-T)/\tau}\,dt}$$

where the decay time scale τ is estimated from scaling as $\tau = \frac{z_{mld}^2}{\mathrm{k}_{mld}}$ and the cut–off time, T^* is $T^* = \tau \ln 10$ (*i.e.* integrate back until the exponential decays to $\frac{1}{10}$). For the ASIAEX

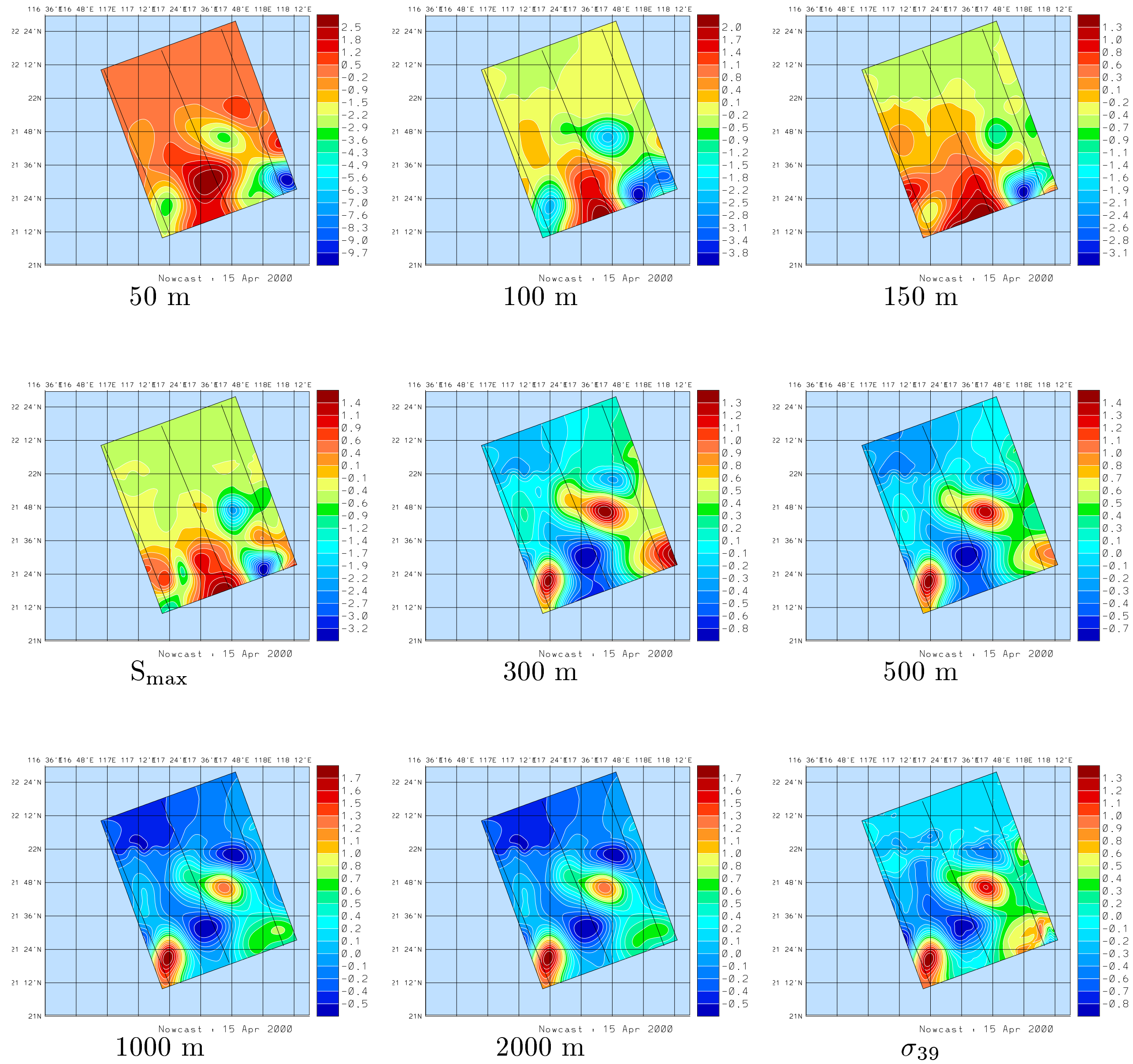

Figure 20 : Level of no-motion comparison 1. The initial transport streamfunction (Sv) resulting from different choices of the reference surface.

data with a mean mixed layer depth of 25.8907 (m) and a chosen mixed layer mixing coefficient of $k_{mld} = 10^4 cm^2/s$ we see a decay scale of roughly 11 minutes and a cut-off time of roughly 26 minutes (*i.e.* nearly interpolating in time).

We then apply a Least-Squares minimization to the mixed layer depths to best fit κ_E, M & N (table at beginning of this section and figure 23). For the Ekman model, the Least-Squares minimization produced a simple analytic expression that merely had to be

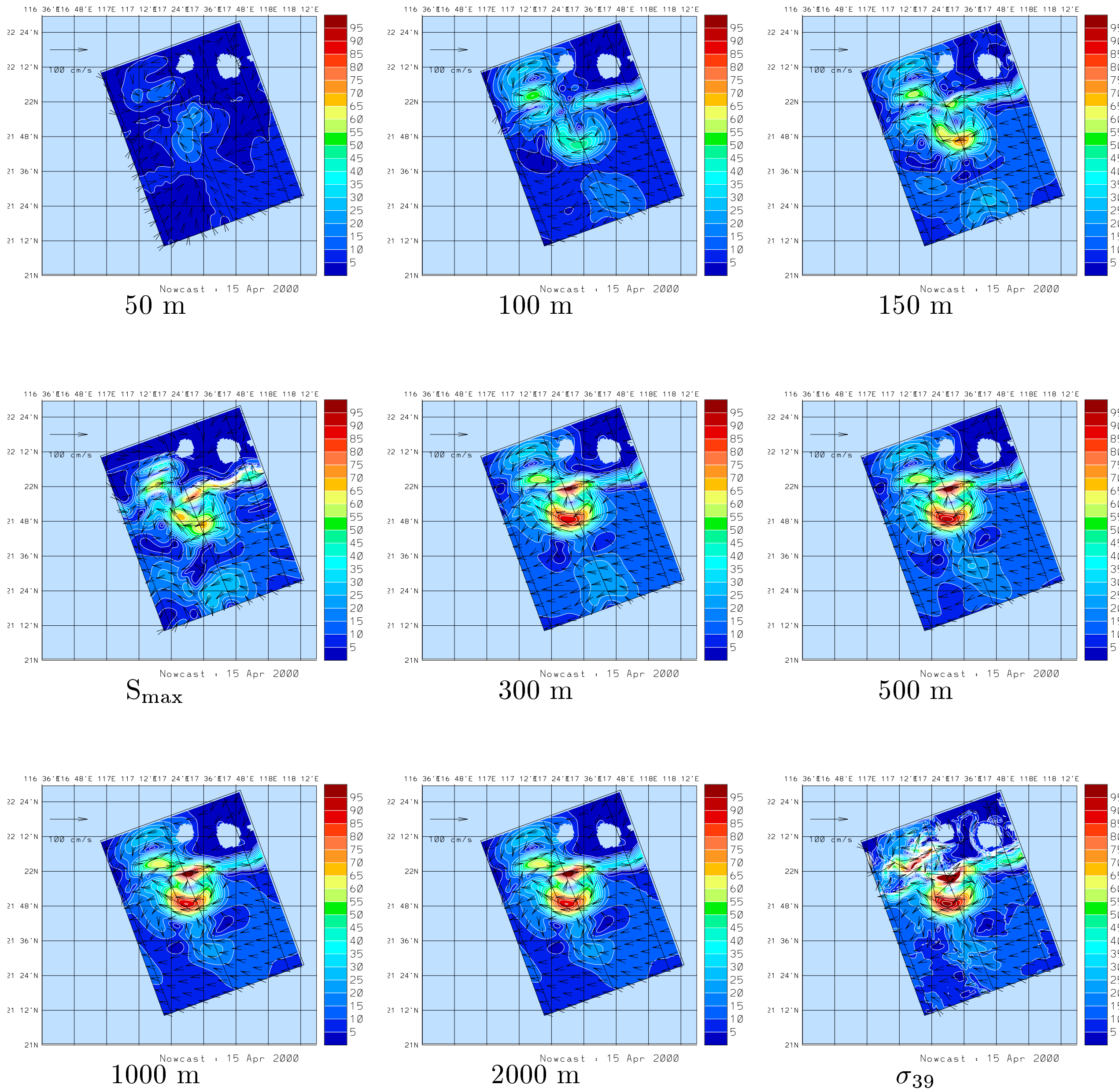

Figure 21 : Level of no-motion comparison 2. The initial velocity (cm/s) at 30m resulting from different choices of the reference surface.

evaluated

$$\kappa_E = \frac{\sum z_{mld} \frac{||\tau||}{\rho f}}{\sum \frac{||\tau||^2}{\rho^2 f^2}}$$

While the Least-Squares minimization of the Niiler-Kraus model resulted in a sensitive, nonlinear vector function that was solved with Newton iteration. In order to obtain a "global" minimum, chose different initial guesses for N that spanned the valid range, [0, 1], in steps of 0.01. Although the Ekman model had slightly better statistics, the

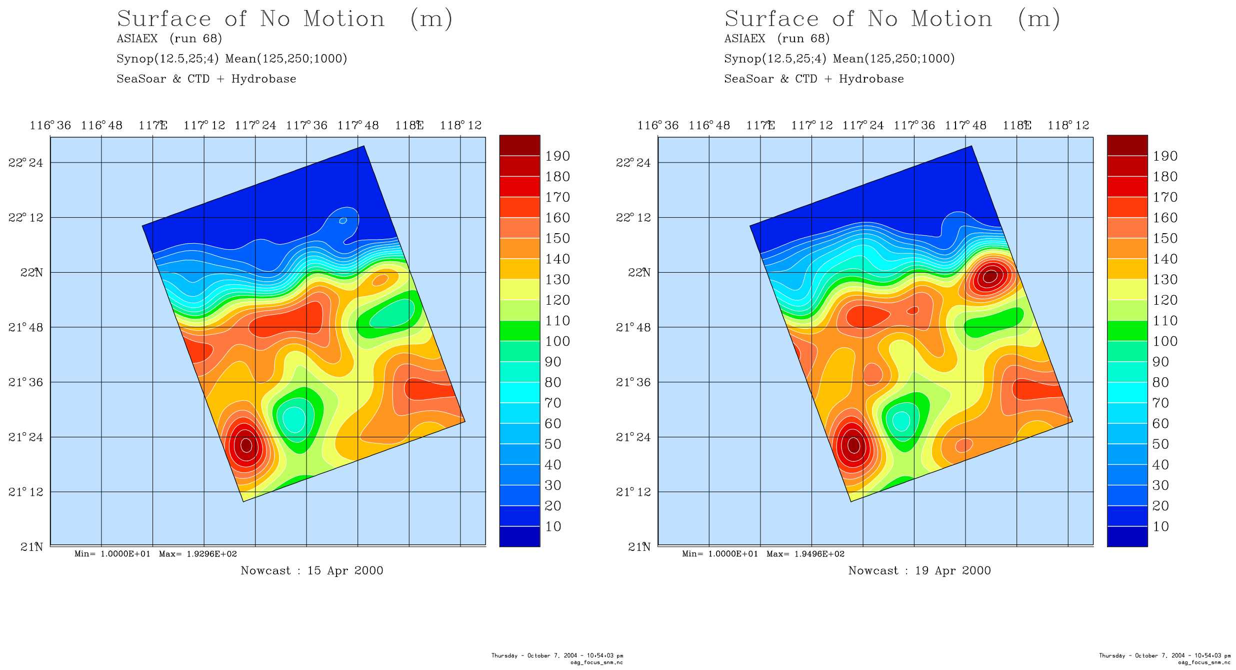

Figure 22 : Surface of no motion. Left: surface at 15 April 2000; Right: surface at 19 April 2000.

Niiler-Kraus was chosen as it better represented the variability. In addition to the fitted parameters shown in figure (23), this examination yielded a minimum MLD of 1.2335(m), a maximum MLD of 70.1193(m) and a mean MLD of 25.8907(m). The first 2 values were used to constrain the computed MLD. The third value was used as the "fall-back" value (the value used when the Niiler-Kraus scheme would degenerate into division by zero).

Central simulation

In the central simulation, the CTD data is not assimilated, but reserved as a check (figures 24–34). The model is run for 5 days with a 150 second time step. The Shapiro filter parameters for internal velocity and tracers are (8,1,1) while the vorticity and transport are filtered with (4,1,1). The boundary conditions are Orlanski radiation on internal mode velocity and "Provided-Orlanski" on tracers, vorticity and transport (Perkins *et al.*, 1997). "Provided-Orlanski" simply means that the Orlanski algorithm is applied to the difference between the model fields and the provided boundary data (*i.e.* radiate out the difference). Pacanowski-Philander mixing is used in the vertical with momentum mixing (FKPM,WVMIX,VVCLIM) of (0.1,50,0.1); tracer mixing (FKPH,WDMIX,VDCLIM) of (0.01,34,0.01) and maximal Richardson factor (FRICMX=25). The bottom friction has a vertical decay scale of 1.5 levels and a temporal decay scale of 10800 (s).

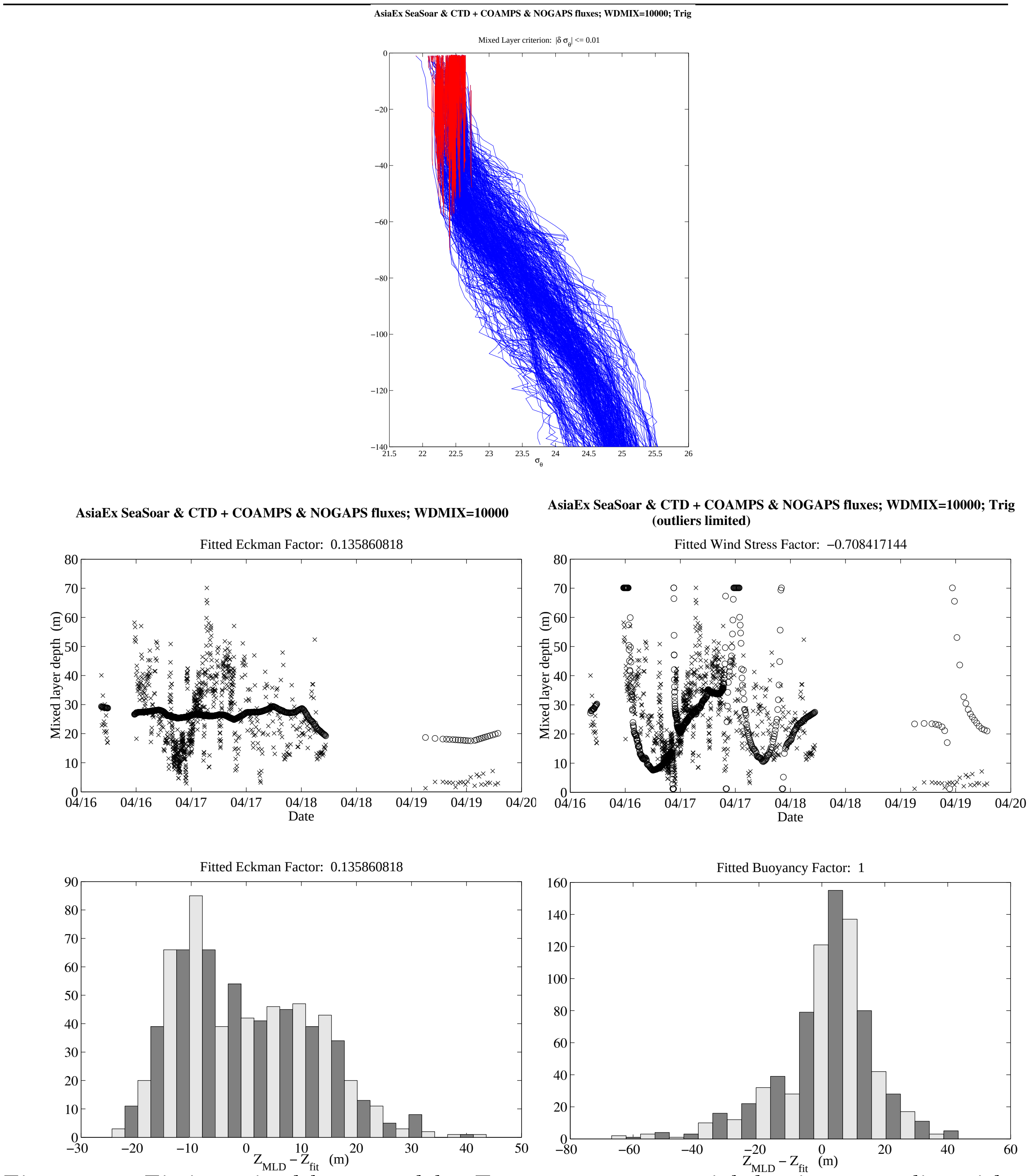

Figure 23 : Fitting mixed layer models. Extreme top: potential density anomalies with portions in mixed layer in red. Left, fitting Ekman model; Right, fitting Niiler-Kraus model. Middle row, data mixed layer depth (x) and fitted mixed layer depths (o).

Appendix I: Surface Bulk Formulae

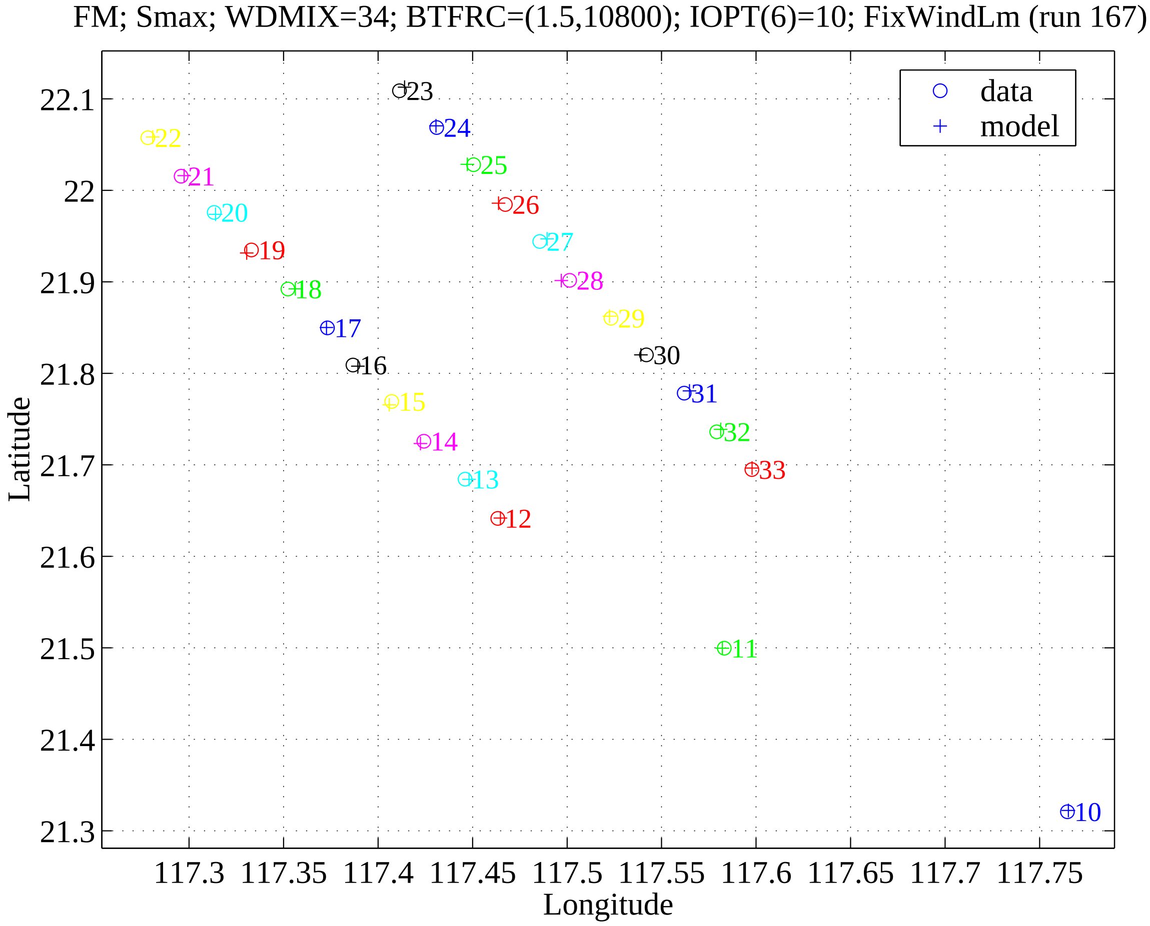

Figure 24 : Simulation-CTD comparison. The locations of the CTD data (circles), the extracted model profiles (pluses) and the associated cast identifiers.

Solar Radiation

Incoming, top of the atmosphere

As mentioned before, the atmospheric fields need to be augmented with the incoming solar radiation. The solar radiation is constructed from an empirical formula (Peixoto & Oort, p98–99) with a correction added for the cloud cover. The instantaneous incoming radiation, Q_0 is given by,

$$Q_0 = \max\left[S\left(\frac{d_m}{d}\right)^2 (\sin\phi\sin\delta + \cos\phi\cos\delta\cos h)\ ,\ 0\right]$$

where

- S is the solar constant, the amount of solar radiation per unit area per unit time at the earth's mean distance from the sun. $S = 1360$ W/m^2.
- d_m is the earth's mean distance from the sun.
- d is the earth's current distance from the sun.
- ϕ is the latitude (radians) at which to evaluate Q_0.

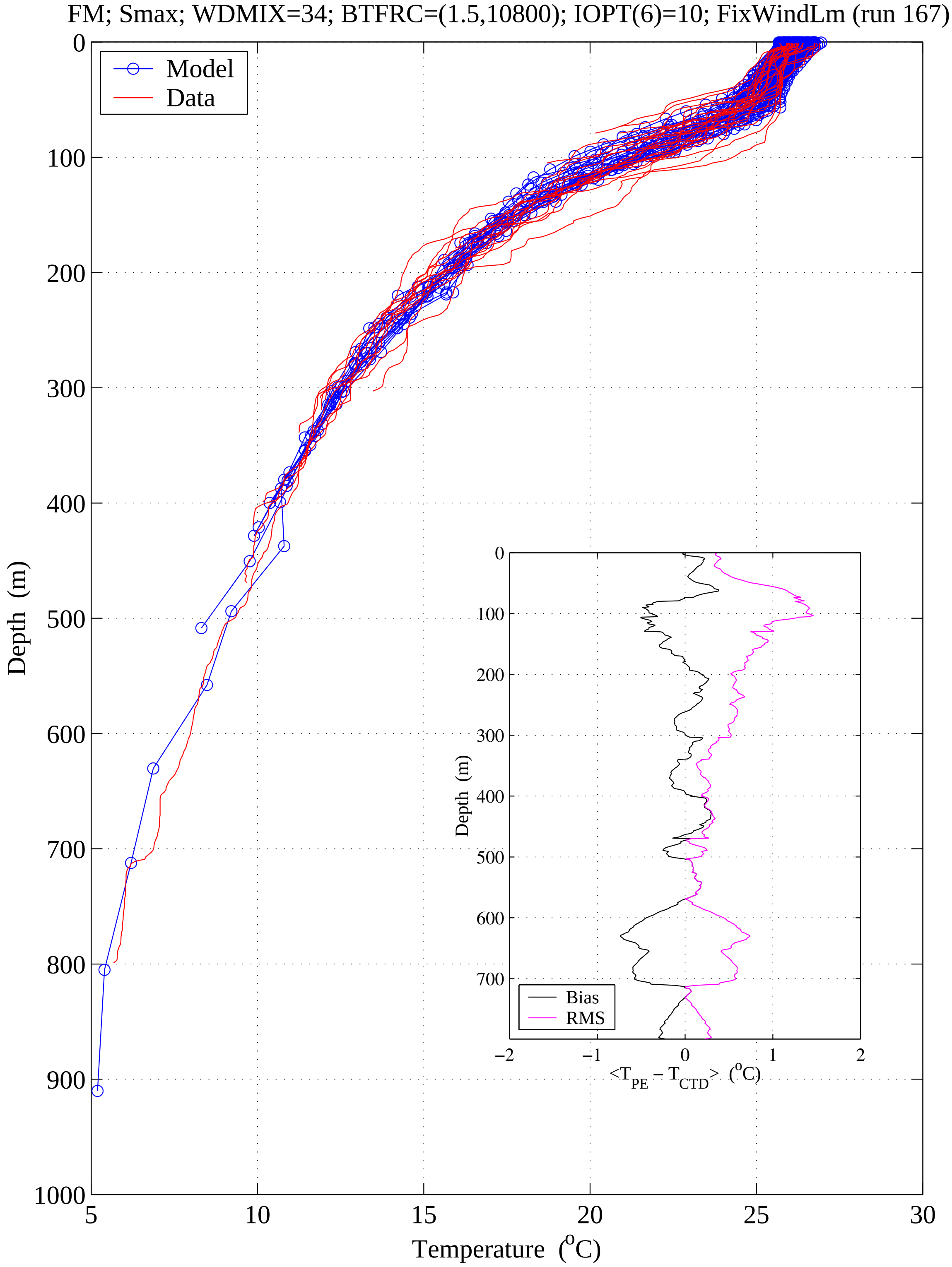

Figure 25 : Simulation-CTD comparison. The model temperatures and CTD temperatures overlaid over entire depth range.

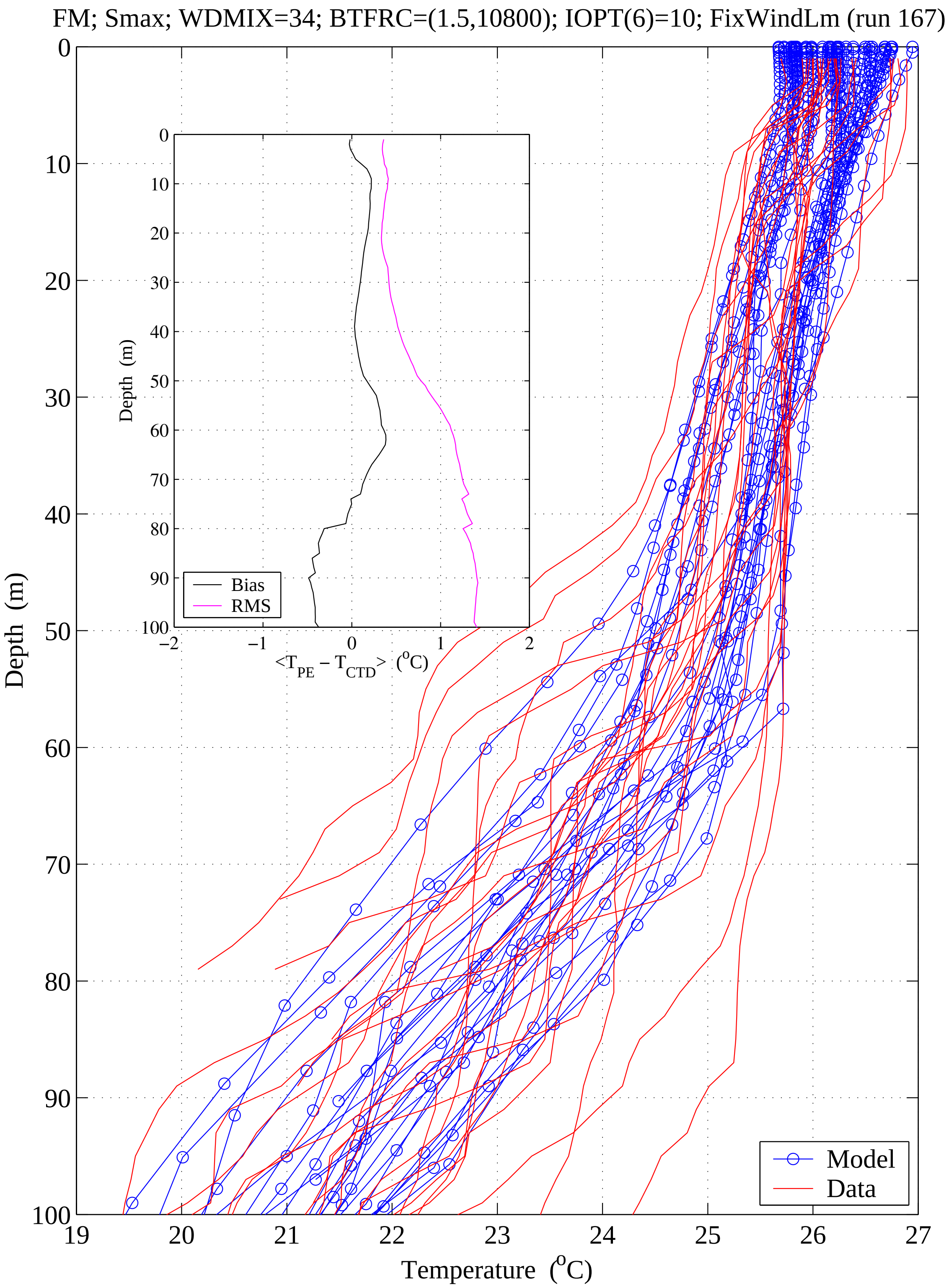

Figure 26 : Simulation-CTD comparison. The model temperatures and CTD temperatures overlaid over near surface region.

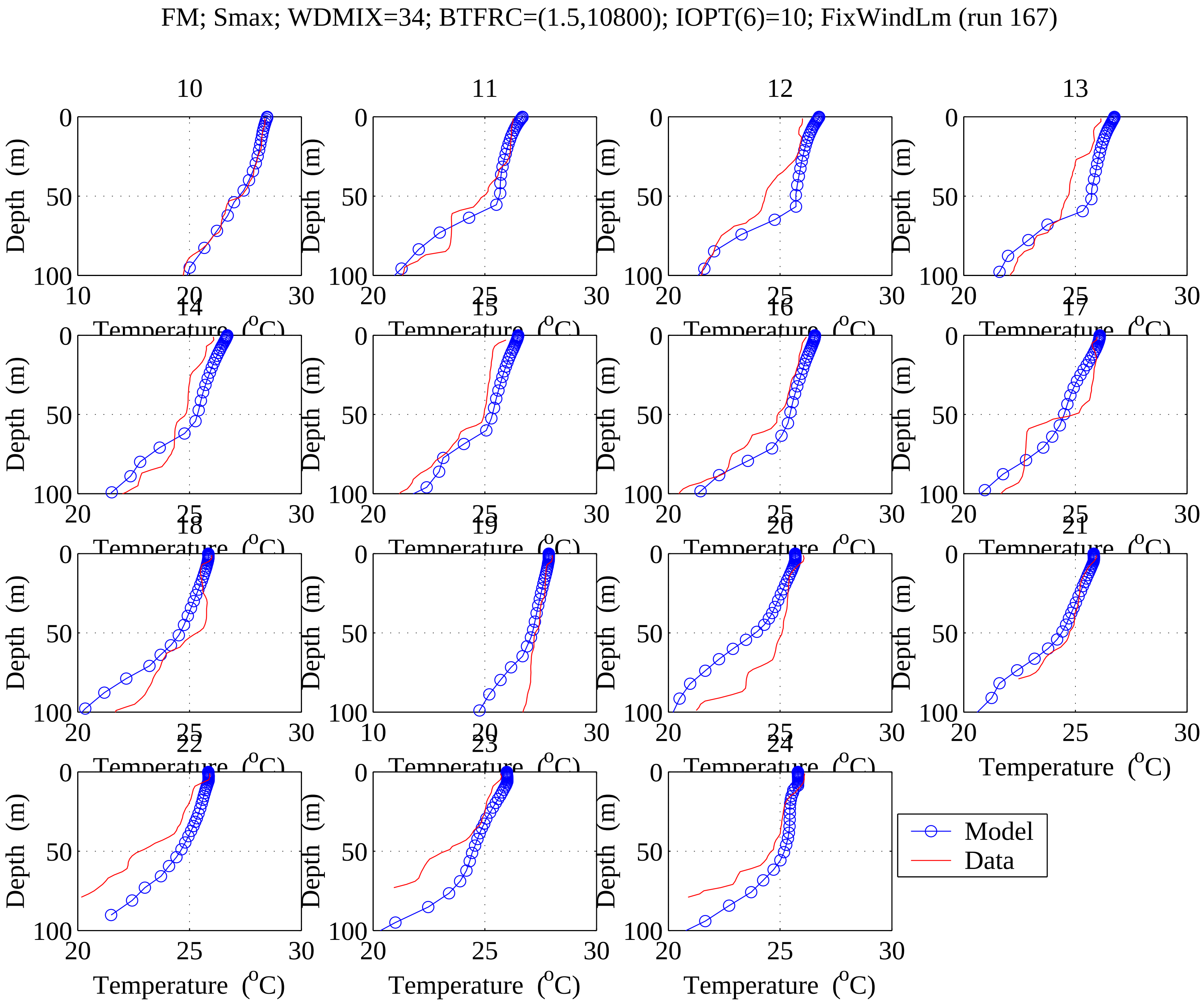

Figure 27 : Simulation-CTD comparison. Individual model temperatures and CTD temperatures overlaid over near surface region.

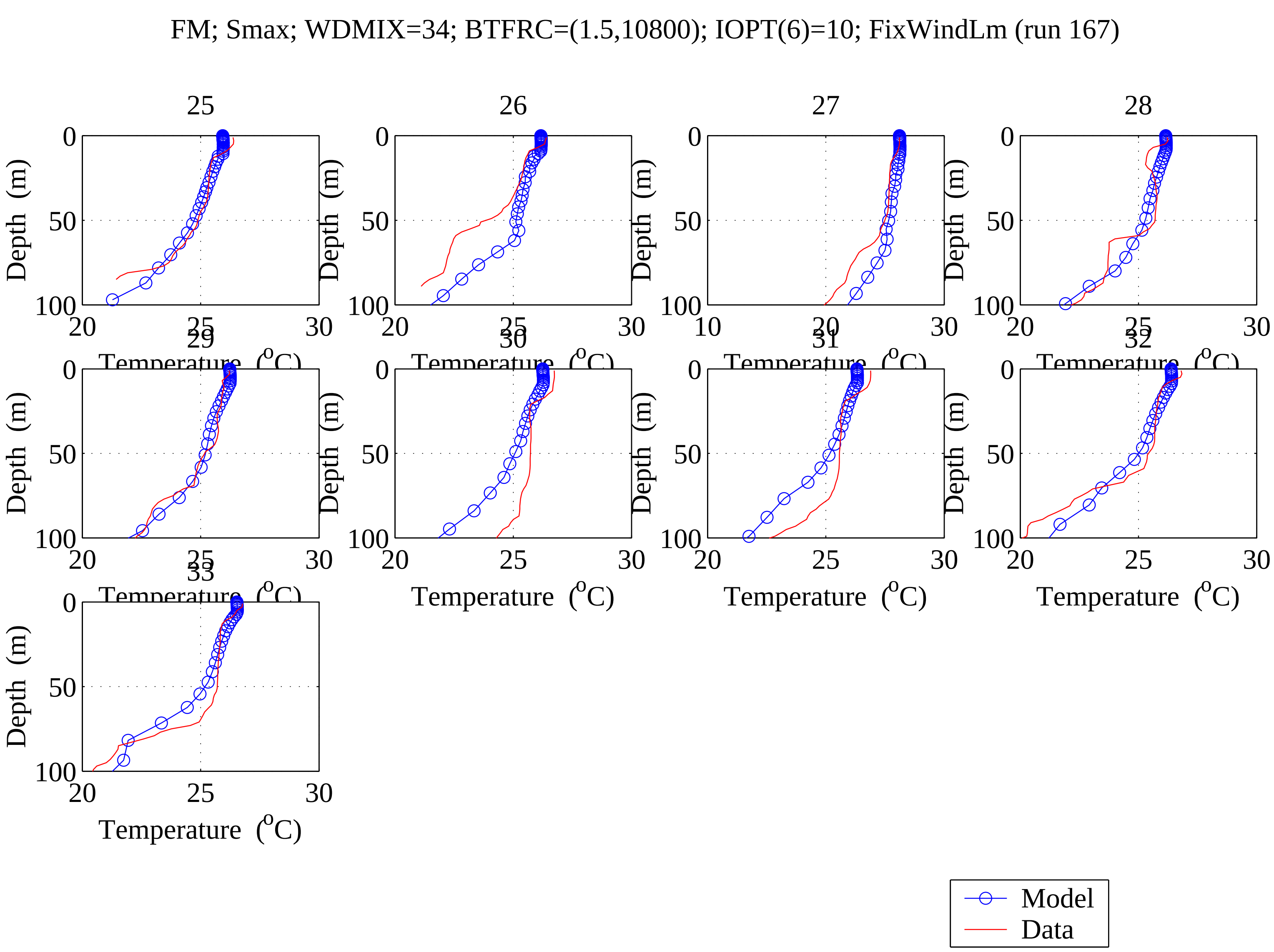

Figure 28 : Simulation-CTD comparison. Individual model temperatures and CTD temperatures overlaid over near surface region.

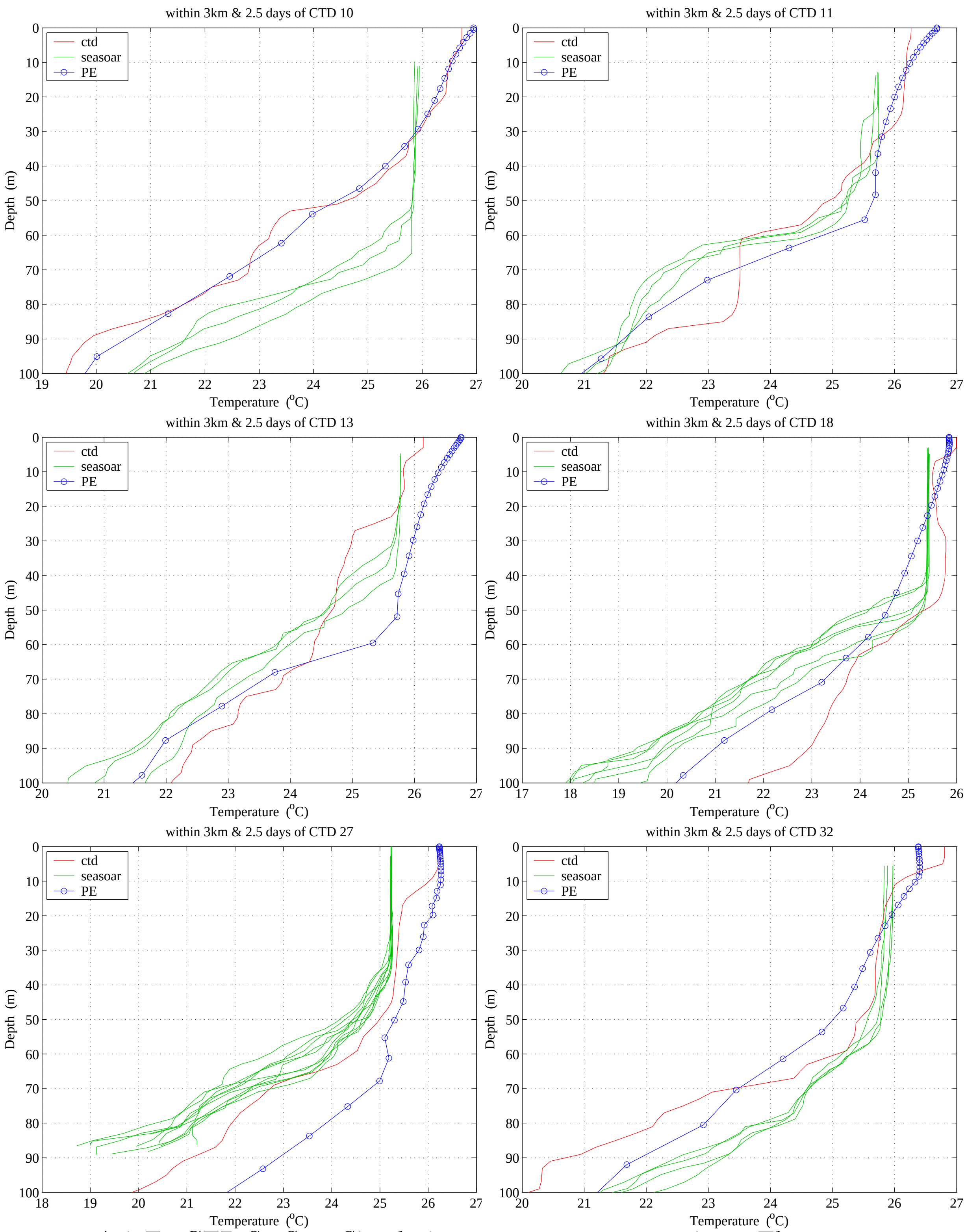

Figure 29 : AsiaEx CTD-SeaSoar-Simulation temperature comparison. The temperature from any CTD which has SeaSoar profiles within 3km and 2.5 days is plotted along with the nearby SeaSoar temperatures and the PE temperature extracted to mimic the CTD.

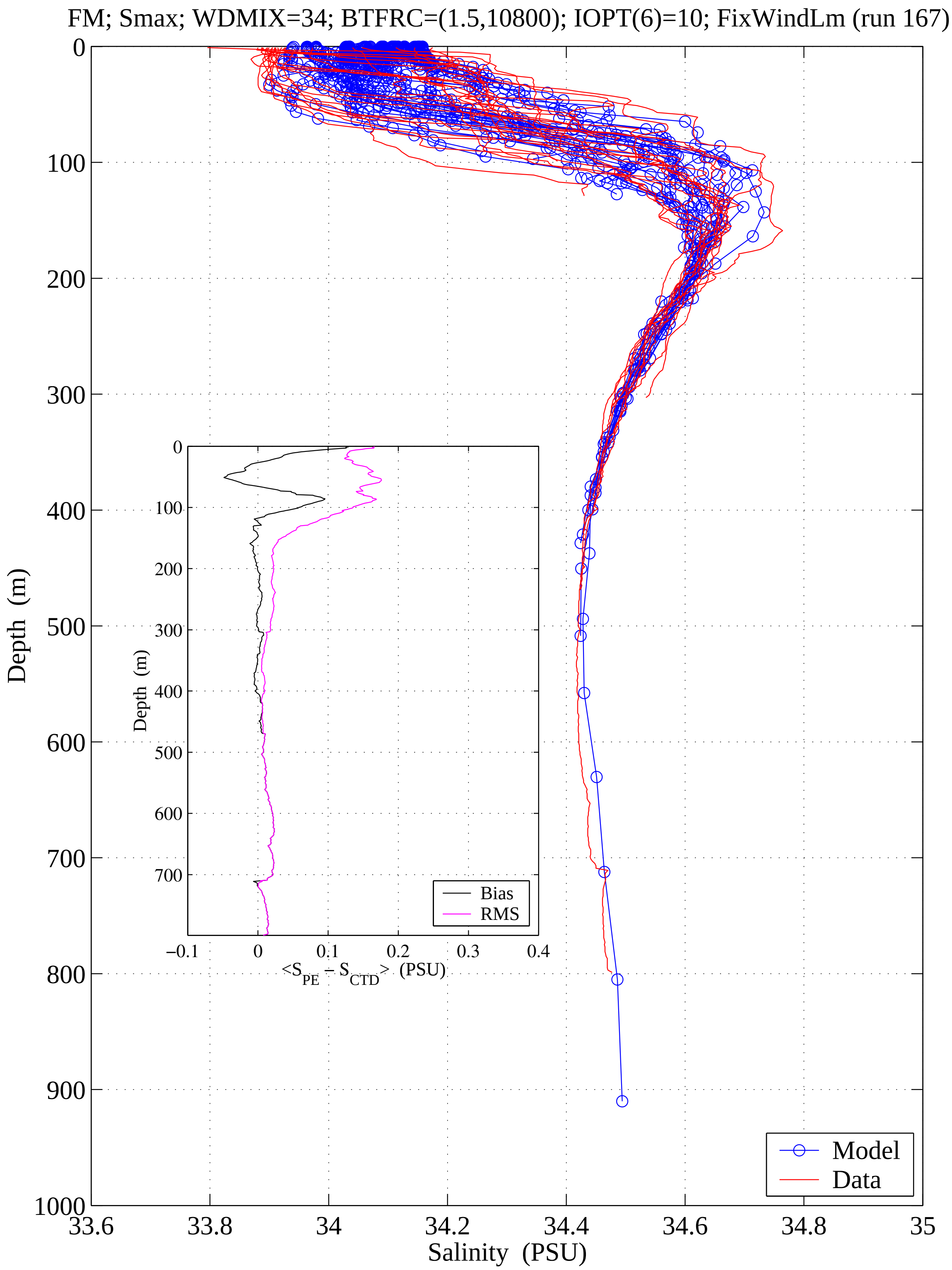

Figure 30 : Simulation-CTD comparison. The model salinities and CTD salinities overlaid over entire depth range.

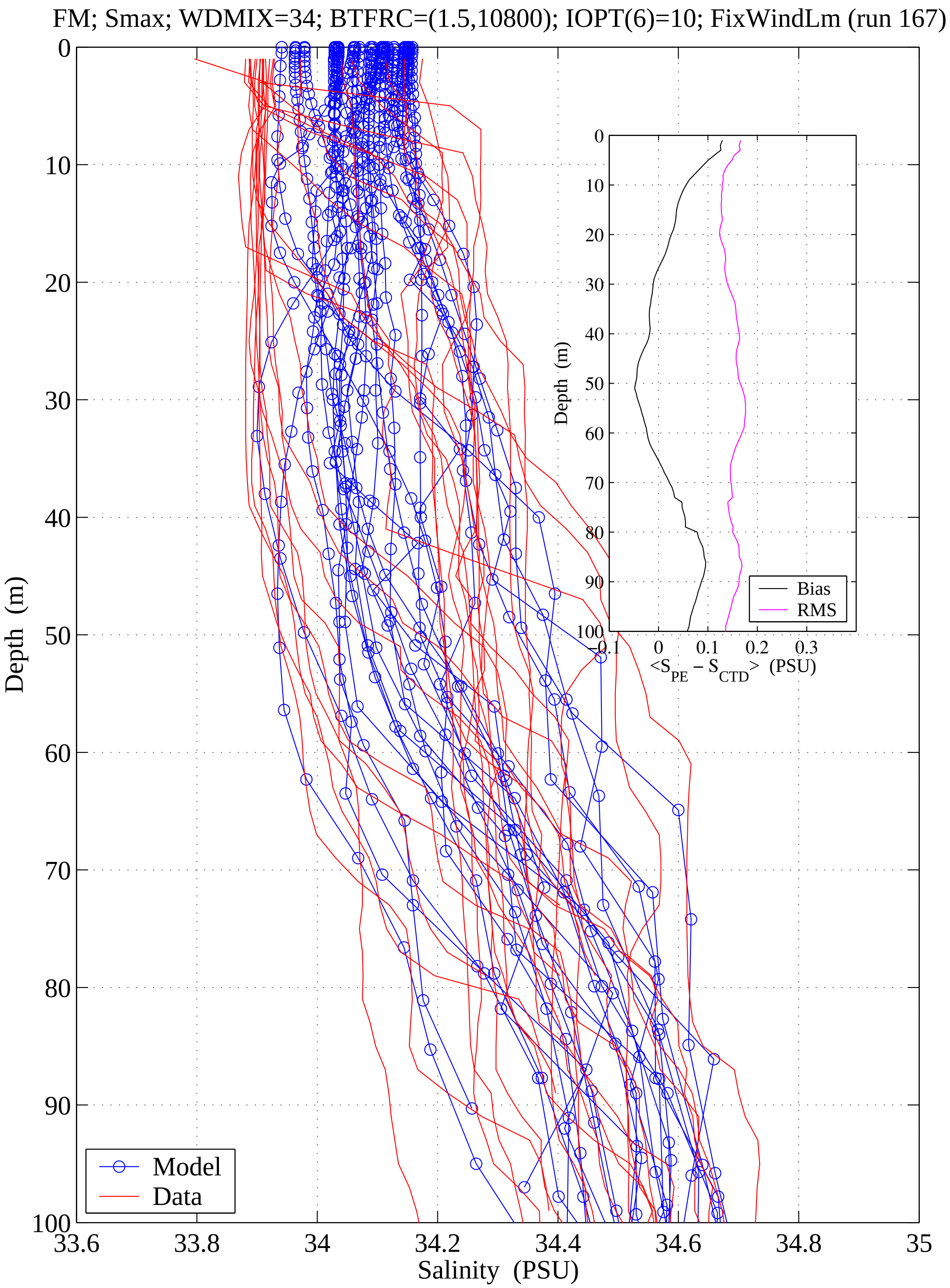

Figure 31 : Simulation-CTD comparison. The model salinities and CTD salinities overlaid over near surface region.

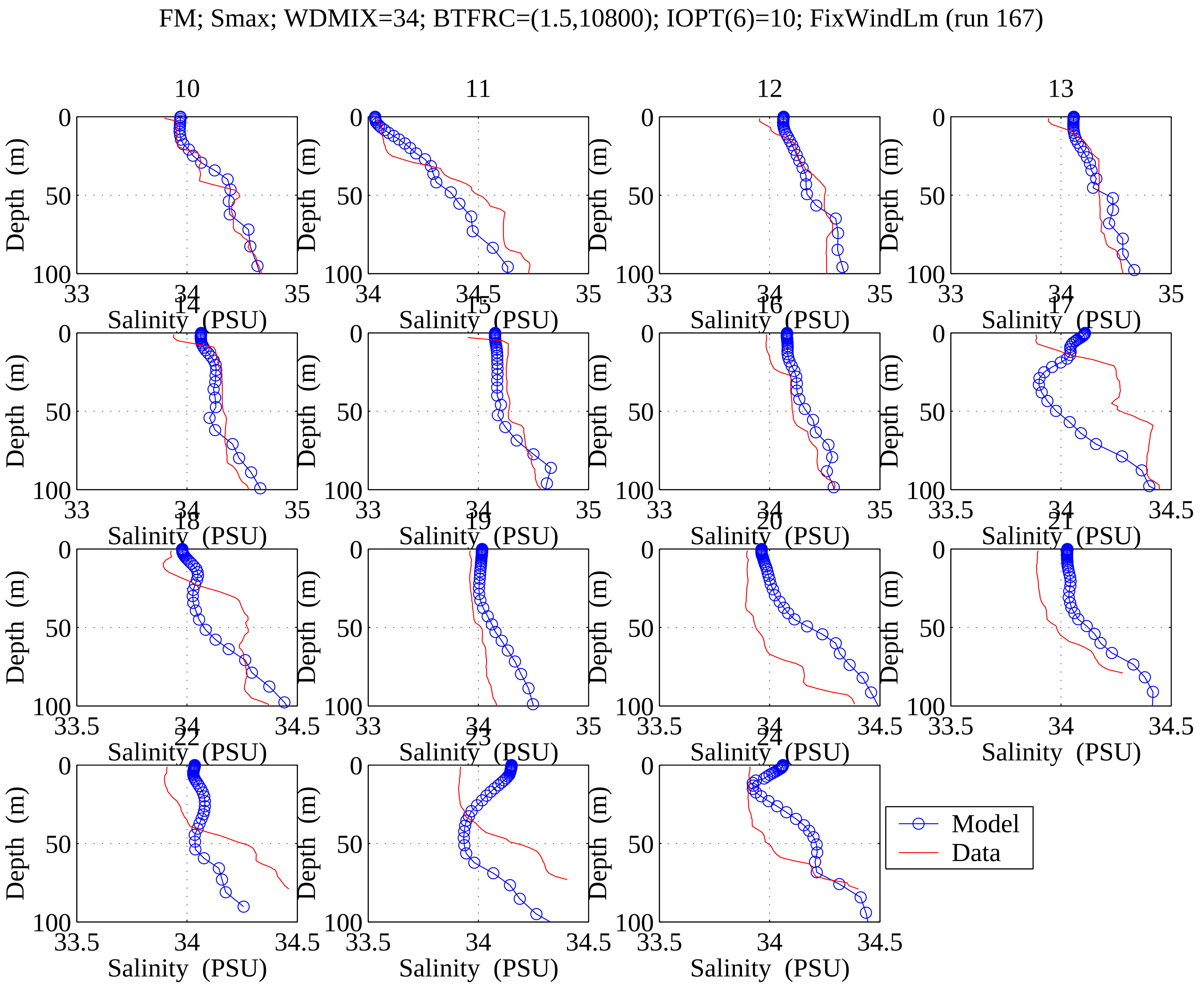

Figure 32 : Simulation-CTD comparison. Individual model salinities and CTD salinities overlaid over near surface region.

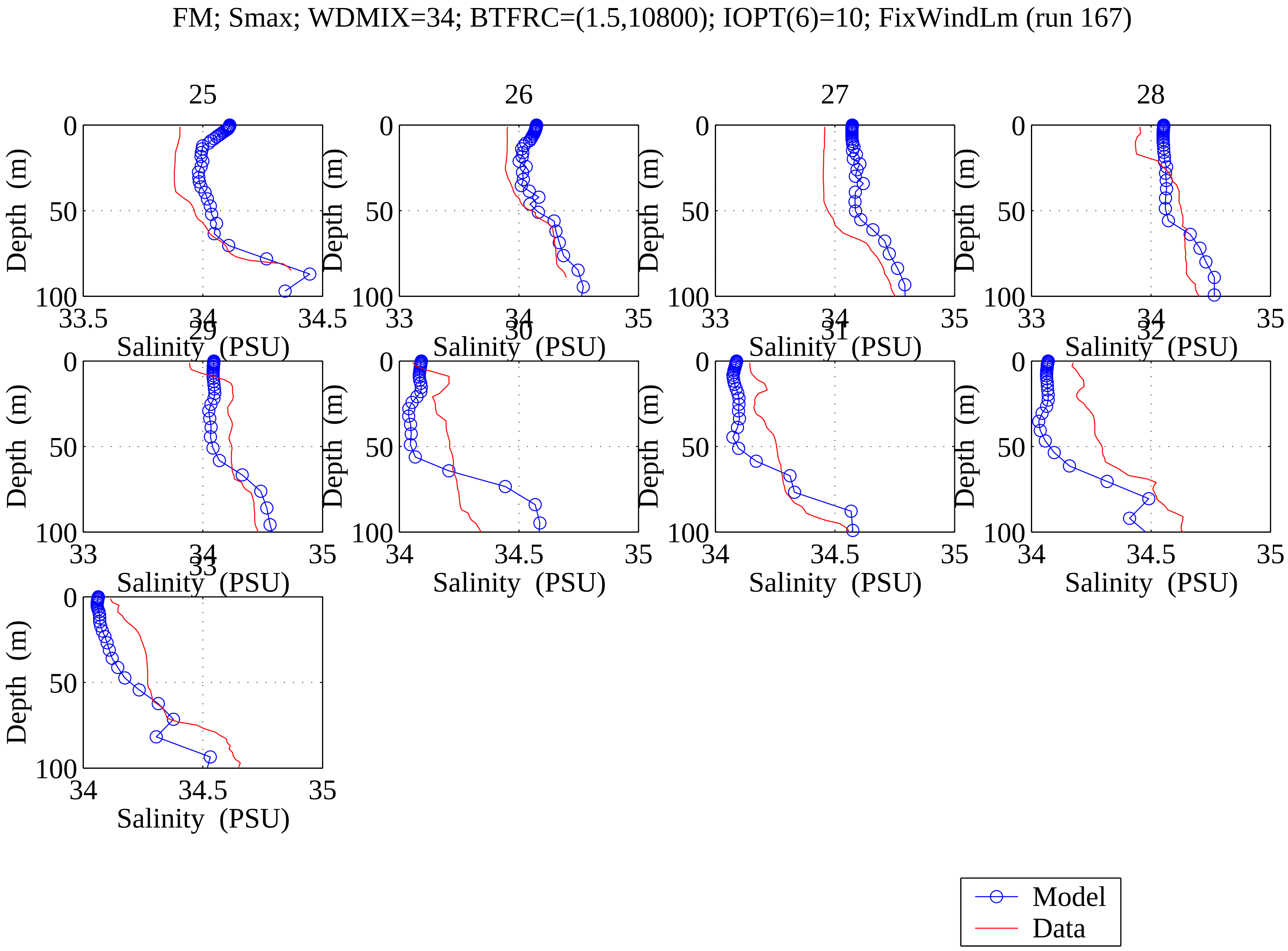

Figure 33 : Simulation-CTD comparison. Individual model salinities and CTD salinities overlaid over near surface region.

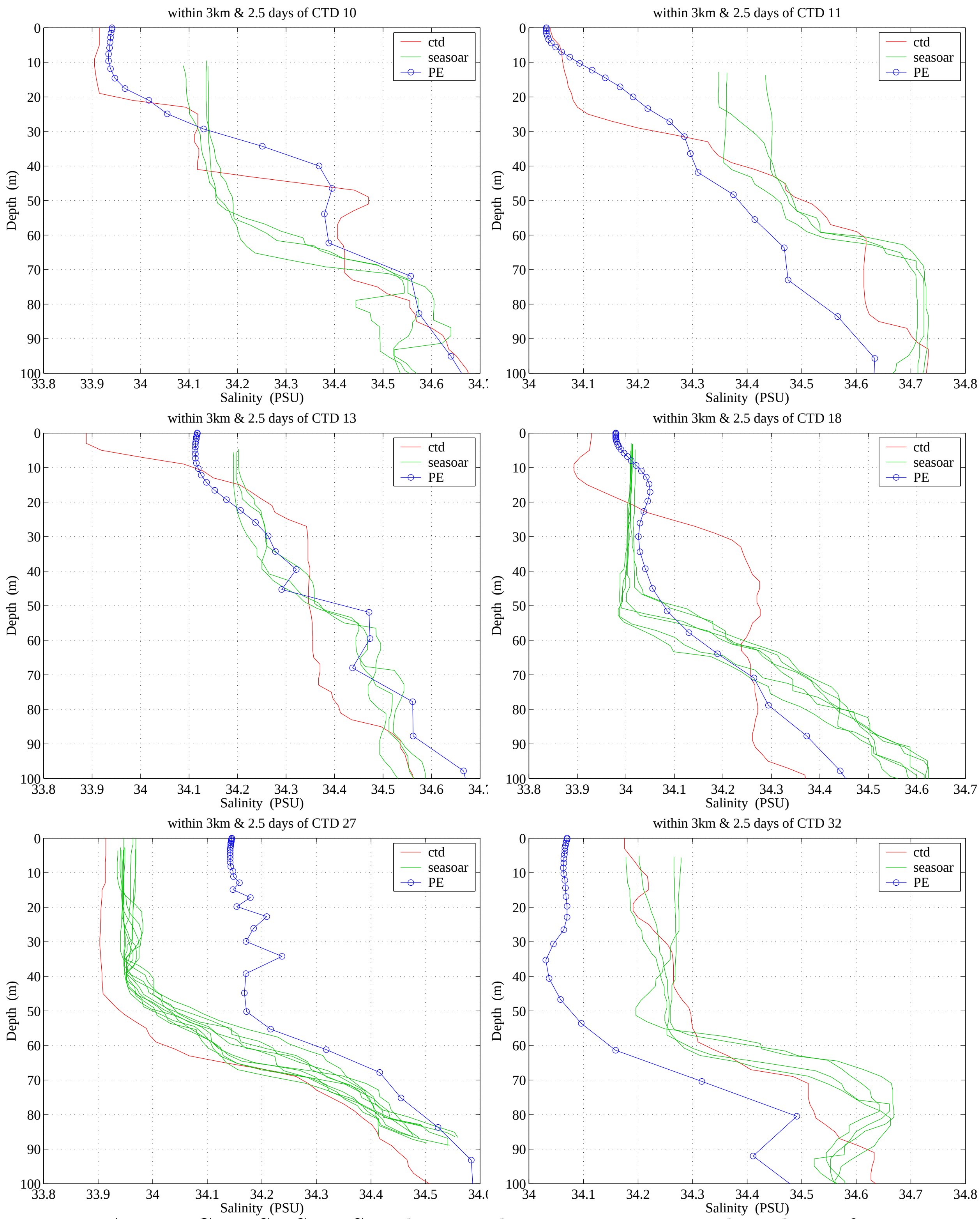

Figure 34 : AsiaEx CTD-SeaSoar-Simulation salinity comparison. The salinity from any CTD which has SeaSoar profiles within 3km and 2.5 days is plotted along with the nearby SeaSoar salinities and the PE salinity extracted to mimic the CTD.

δ is the solar declination.

h is the hour angle, having a value of zero at local solar noon.

The square of the ratio of the earth's mean distance to the current distance is modeled assuming a cosine relation with the closest approach on January 6.

$$\left(\frac{d_m}{d}\right)^2 \approx 1 + 0.035 \cos\left[\frac{2\pi}{365}(6 - yd)\right] \quad ,$$

where

yd is the year–day (including fractional part).

The solar declination is modeled assuming a cosine relation with a declination of -23.45° on December 21.

$$\delta \approx \frac{-23.45\pi}{180} \cos\left[\frac{2\pi}{365}(355 - yd)\right] \quad .$$

Finally, to evaluate the hour angle, h, we make the assumption that along the Prime Meridian, local solar noon always occurs at 1200Z. Then

$$h = 2\pi\left(\frac{t_{GMT}}{24} + \frac{\psi}{360} - \frac{1}{2}\right)$$

where

t_{GMT} is the (decimal) time of day, Greenwich Mean Time, at which Q_0 is evaluated. (e.g. at 1415 GMT, $t_{GMT} = 14.25$)

ψ is the longitude (degrees) at which Q_0 is being evaluated

Incoming, into top of the ocean

The next step is estimating the amount of radiation that reaches the ocean surface. The two numbers used in this estimate are:

- 76% of the radiation penetrates the atmosphere on a cloudless day[2].
- Peak cloudiness can block up to 70% of the incoming radiation. (Peixoto & Oort, p103)

Mathematically, this is modeled as

$$Q_I = 0.76 Q_0 (1 - 0.7C)$$

where

C is the fractional cloud cover (nondimensional) obtained from NOGAPS[3]

[2] Looking at Gill (p10) or Peixoto & Oort (p92), I'd have said 74%. This is an admittedly insignificant correction.

[3] The cloud cover is interpolated to the COAMPS grid. This produces some small excursions outside the valid range [0, 1], which have to be clipped immediately upon being read.

Net Heat Flux

The net heat flux into the ocean, Q, is given by

$$Q = Q_I - Q_B - Q_L - Q_S$$

where

Q_I is the rate of absorption of solar radiation (W/m^2), described above
Q_B is the upward flux of long–wave radiation (W/m^2)
Q_L is the upward latent heat flux (W/m^2).
Q_S is the upward sensible heat flux (W/m^2).

These components are computed from a combination of empirical formulae and atmospheric analysis and forecast fields produced by COAMPS, NOGAPS and TOPS. The remainder of this section describes the formulae used and how the atmospheric data are incorporated for Q_B, Q_L and Q_S.

Long–wave Radiation

The upward long–wave radiation is the blackbody radiation formula with corrections for (a) departure of the ocean from blackbody behavior (0.985), (b) back radiation in the absence of clouds and (c) the effects of clouds (Gill, p34).

$$Q_B = 0.985\sigma\left(T_{sst} + 273.15\right)^4\left(0.39 - 0.05\sqrt{e_a}\right)\left(1 - 0.6C^2\right)$$

where

σ is the Stefan constant $5.67\,(10^-8)$ $(\mathrm{W\,m^{-2}\,K^{-4}})$.
T_{sst} is the sea surface temperature (°C) obtained from TOPS[4]
e_a is the vapor pressure of water (mb) at the standard height

The vapor pressure is computed from (Gill, p605)

$$e_a = \frac{Pq_a}{\epsilon + (1 - \epsilon)q_a}$$

where

P is the pressure (mb) obtained from COAMPS[5]
q_a is the specific humidity (nondimensional)
ϵ is the ratio of the molecular weight of water (18.016) to the molecular weight of air (28.966). $\epsilon = 0.62197$

The specific humidity is computed from (Gill, p605)

$$q_a = \frac{R_h q_{sat}}{1 - q_{sat} + R_h q_{sat}}$$

[4] This is actually coming in as Kelvin, but is being converted immediately after being read.

[5] This is actually coming in as Pascal, but is being converted immediately after being read.

where

R_h is the relative humidity (nondimensional) obtained from COAMPS

q_{sat} is the saturation specific humidity (nondimensional)

The saturation specific humidity is computed from (Gill, p605)

$$q_{sat} = \frac{\epsilon \frac{e_{sat}}{P}}{1 - (1 - \epsilon) \frac{e_{sat}}{P}}$$

where

e_{sat} is the saturation vapor pressure (mb)

The saturation vapor pressure is computed from (Gill, p606)[6]

$$e_{sat} = 10^{\left(\frac{0.7859 + 0.03477 T_{air}}{1 + 0.00412 T_{air}} \right)}$$

where

T_{air} is the air temperature (^{o}C) obtained from COAMPS[7]

Latent Heat Flux

The upward latent heat flux is the product of the evaporation rate, E, and the latent heat of vaporization, L_V

$$Q_L = L_V E \quad .$$

The evaporation rate ($\mathrm{kg\, m^{-2}\, s^{-1}}$) is given by (Gill, p30)

$$E = \rho_{air} c_e U \left(q_{sat} - q_a \right)$$

where

ρ_{air} is the density of air ($\mathrm{kg/m^3}$)

c_e is the Dalton number, $1.5 \left(10^{-3}\right)$ (nondimensional)

U is the 10m wind speed (m/s) obtained from COAMPS

The density of air is found from (Gill, p41)

$$\rho_{air} = \frac{100P}{RT_{air_V}}$$

where the 100 is a conversion from millibar to $\mathrm{N/m^2}$,

R is the gas constant for dry air[8], 287.04 $\mathrm{J\, kg^{-1}\, K^{-1}}$

T_{air_V} is the virtual air temperature (K), the temperature that dry air would need to have at the given pressure to have the same density as moist air.

---

[6] Looking at Gill (p606), the saturation pressure given here should probably be multiplied by $0.98 \left[1 + 10^{-6} P \left(4.5 + 0.0006 T_{air}^2\right)\right]$ (eq A4.6, A4.7 and note e)

[7] This is actually coming in as Kelvin, but is being converted immediately after being read.

[8] R is related to the universal gas constant, R_*, by the relation $R = \frac{R_*}{m_a}$ where m_a is the molecular weight of air and $R_* = 8314.16 \mathrm{J\, kmol^{-1}\, K^{-1}}$

The virtual air temperature is found from (Gill, p41)[9]

$$T_{air_V} = (T_{air} + 273.15)\,(1 + 0.6078 q_a)$$

The latent heat of vaporization ($\mathrm{J\,kg^{-1}}$) is found from (Gill, p607)

$$L_V = 2.5008\left(10^6\right) - 2.3\left(10^3\right) T_{air}$$

Sensible Heat Flux

The upward sensible heat flux is found from (Gill, p30)

$$Q_s = \rho_{air} c_{p_{air}} c_H U \left(T_{sst} - T_{air}\right)$$

where

$c_{p_{air}}$ is the heat capacity per unit mass of air ($\mathrm{J\,kg^{-1}\,K^{-1}}$)

c_H is the Stanton number (nondimensional), $8.3\left(10^{-4}\right)$ for stable conditions[10].

The capacity per unit mass of air is found from (Gill, p43)[11]

$$c_{p_{air}} = 1004.6(1 + 0.8375 q_a)$$

Water Flux

The surface flux of water out of the ocean, F_{H_2O} (cm/day), is given by the difference of evaporation and precipitation

$$F_{H_2O} = \frac{86400 \cdot 100}{\rho_{H_2O}} E - P_{rain}$$

where 86400 is the conversion from days to seconds, 100 is the conversion from meters to centimeters,

ρ_{H_2O} is the density of water, 1000 kg/m^3

P_{rain} is the precipitation rate (cm/day) obtained from COAMPS[12]

Wind Stress

The wind stress, $\vec{\tau}$ (dynes/cm^2), is given by (Pond & Picard, p108)

$$\vec{\tau} = 10 C_D \tilde{\rho}_{air} ||\vec{U}|| \vec{U}$$

where the 10 is simply a conversion factor from N/m^2 to dynes/cm^2,

$\tilde{\rho}_{air}$ is the density of air[13] , 1.3 kg/m^3

C_D is the drag coefficient, 0.0014 (nondimensional)[14]

---

[9] Before substituting the number, Gill expresses this as $T_{air_V} = (T_{air} + 273.15)\left(1 - q_a + \frac{q_a}{\epsilon}\right)$

[10] For unstable conditions, $1.1\left(10^{-3}\right)$. Gill also suggests that alternative formulations are available.

[11] Before substituting the numbers, Gill expresses this as $\frac{7}{2} R \left(1 - q_a + \frac{8 q_a}{7\epsilon}\right)$.

[12] This is actually coming in as $\frac{\mathrm{kg}}{\mathrm{m^2 (12hr)}}$, but is being converted immediately after being read. There are many small values of -0.00254, which are being reset to zero.

[13] I find it curious that we make the effort to calculate an ideal gas type value for the density of air in the latent heat flux and take a canonical value here.

[14] Pond & Picard (p 135-138) also indicate that the drag coefficient is an increasing function of wind speed, varying by a factor of 2–3. This should be researched.

References

Curry, R. *HydroBase2* Download Database.
http://www.whoi.edu/science/PO/hydrobase/HB2_DownloadDatabaseMain.htm

Gill, A.E. (1982) Atmosphere–Ocean Dynamics. Academic Press. New York. 662 pp.

Master Environmental Library (MEL).
https://mel.dmso.mil/

Niiler, P.P. & E.B. Kraus (1977) One-Dimensional Models of the Upper Ocean. in *Modelling and Prediction of the Upper Layers of the Ocean.* E.B. Kraus (ed.) Pergamon Press. pp 143–172.

Peixoto, J.P. & A.H. Oort (1992) Physics of Climate. American Institute of Physics. New York. 520 pp.

Perkins, A.L., L.F. Smedstad, D.W. Blake, G.W. Heburn, & A.J. Wallcraft (1997) A new nested boundary condition for a primitive equation ocean model. *J. Geophys. Res.*, **102**(C2). 3483–3500.

Pond, S. & G.L. Pickard (1983) Introductory Dynamical Oceanography. 2nd ed. Pergamon Press. Oxford. 349 pp.